Palaeogeography, Palaeoclimatology, Palaeoecology
October 2009, Volume 281, Issues 1-2, Pages 66-78
http://dx.doi.org/10.1016/j.palaeo.2009.07.012

What forced the collapse of European ice sheets during the last two glacial periods (150 ka B.P. and 18 ka cal B.P.)? Palynological evidence

A. Penaud[a, *], F. Eynaud[a], J.L. Turon[a], S. Zaragosi[a], B. Malaizé[a], S. Toucanne[a] and J.F. Bourillet[b]

[a] Université Bordeaux 1, Avenue des Facultés, CNRS, UMR 5805-EPOC, F-33405 Talence, France
[b] IFREMER, Département Géosciences Marines, Laboratoire Environnements Sédimentaires, BP 70-29280 Plouzané, France

*: Corresponding author : A. Penaud, Tel.: +33 540 008 832; fax: +33 556 840 848, email address : a.penaud@epoc.u-bordeaux1.fr

Abstract:

We present a new marine palynological record from the temperate North-eastern Atlantic (core MD03-2692, Celtic–Armorican margin) in the area of influence of the 'Fleuve Manche' paleoriver during glacial times. The runoff of this paleoriver was connected to the glacial history of European ice sheets (including the British Irish Ice Sheet—BIIS). Our study conducted on dinoflagellate cysts assemblages over the last 200 ka, associated with quantification of palynological remains reflecting continental influence (pre-Quaternary dinocysts and micro-algae Pediastrum spp. coenobia), yields detailed insights into the sea-surface paleoenvironments of this sector. More specifically, mechanisms responsible for the origin of unusual deposits of laminated sequences found at the end of Marine Isotope Stage (MIS) 2 and within mid-MIS 6 are here constrained. We provide evidence of genetic similarities between fluvial discharges occurring before and during times of deposition of the laminated deposits. Our study clarifies the causes of the collapse of European glaciated systems. At the end of MIS 2, prior to the deposition of the laminated deposits, pleni-oceanic influence characterized by high concentrations of Quaternary dinocysts prevailed, and a dinocyst species tracing the penetration of the warm North Atlantic Drift into the Bay of Biscay is recorded. However, this scenario did not recur prior to the deposition of laminated sediments of mid-MIS 6. In addition, contrary to the laminated deposits found at the end of MIS 2 and directly associated with Termination I, MIS 6 laminae appeared 20 ka earlier than Termination II. Our work shows that, during the penultimate glacial stage, the collapse of mid-latitudes ice sheets around 170 ka B.P. may have immediately followed the MIS 6.5 warming phase. Then, the most important melting event around 150 ka B.P. may be linked to a peak in insolation at 65°N, though less important than those during MIS 6.5 and Termination II.

Keywords: Dinoflagellate cysts; European ice sheets; Celtic–Armorican margin; MIS 2 and MIS 6; Terminations I and II

1. Introduction

Terminations constitute major shifts from glacial to interglacial periods during the late Quaternary. The penultimate and last Terminations (Termination II and Termination I, respectively) recorded off the present-day English Channel (Bay of Biscay), *i.e.* off the 'Fleuve Manche' paleoriver, one of the largest river that ever drained the Western Europe during glacial episodes (Gibbard et al., 1988; Lericolais, 1997; Lericolais et al., 2003; Bourillet et al., 2003; Gupta et al., 2007), have been the subject of several studies (e.g. Zaragosi et al., 2001, 2006; Mojtahid et al., 2005; Eynaud et al., 2007; Toucanne et al., 2008, 2009). These studies demonstrate a close relationship between European continental paleoenvironments and 'Fleuve Manche' runoff. A compilation of several cores in the Celtic sector from 51.7°N to 46.8°N (Eynaud et al., 2007) illustrates the regional occurrence of a peculiar facies at the end of Marine Isotope Stage (MIS) 2 and within mid-MIS 6, consisting in millimetre-scale IRD-rich clay laminae. This facies has been linked to seasonal sedimentary discharges associated with major episodes of seasonal European ice sheets collapse (Mojtahid et al., 2005; Zaragosi et al., 2001, 2006; Toucanne et al., 2009).
Our work brings new information about the sequencing at the origin of the laminated deposits. With a view to improving knowledge of the regional hydrological and oceanographical settings that influenced the dynamics of European ice sheets, we have conducted palynological investigations (including Quaternary and reworked dinoflagellate cysts (dinocysts), coenobia of *Pediastrum* spp.) on long-piston core MD03-2692 retrieved directly off the 'Fleuve Manche' paleoriver. Dinocysts have proved to be very helpful in reconstructing North Atlantic Quaternary paleoenvironments for more than two decades (e. g. Turon, 1984; Turon and Londeix, 1988; Eynaud et al., 2000; de Vernal et al., 2001; Zonneveld et al., 2001; Mudie et al., 2002; de Vernal et al., 2005; Grøsfjeld et al., 2006). Our results are furthermore compared with several other paleoceanographical proxies obtained from the same core (core MD03-2692; Mojtahid et al., 2005; Eynaud et al., 2007; Toucanne et al., 2009). The new dinocyst sequence produced here is then discussed in parallel with a proximal abyssal core MD95-2002 (Eynaud, 1999; Zaragosi et al., 2001). It allows us to discuss in detail for the first time a paleohydrological scenario for MIS 2 termination in this area. Moreover, until now, few studies focussed on MIS 6 detailed sea-surface paleohydrology. Our study constitutes the first detailed dinocyst sequence obtained in the NE Atlantic on the penultimate Glacial Complex (MIS 6) and the following Termination II.

2. Present and past regional setting

2.1. Present environmental context of core MD03-2692

This study is based on a 'Calypso' long piston core MD03-2692 (46°50'N, 9°31'W, 4064 m water depth, 39 m length; Fig. 1), retrieved during the SEDICAR oceanographic cruise of the *RV Marion Dufresne II* (IPEV; Bourillet and Turon, 2003). The site is located in the Bay of Biscay (NE Atlantic), along the Celtic-Armorican margin, in the axis of the 'Fleuve Manche' paleoriver and the Irish Sea. The studied core was retrieved from the Trevelyan Escarpment, a rise 500 meters higher than the abyssal plain in this area. The core is then situated in hemipelagic environments of the Bay of Biscay, far from any turbiditic influences, which makes it suitable for reconstructing paleoenvironmental scenarios throughout the two last glacial periods. This hemipelagic sequence has provided a high resolution paleoceanographic record extending back to about 340 ka (*i.e.* MIS 10) (Mojtahid et al., 2005).

Four deep water masses control present-day sedimentation (Frew et al., 2000): the Lower Deep Water (LDW, abyssal water mass), overlain by the Northeast Atlantic Deep Water (NEADW, 2 800 m depth), the Labrador Sea Water (LSW, 1 500 m depth) and the Mediterranean Outflow Water (MOW, 800 m depth). Surface waters derive from the North Atlantic Drift (NAD), the major surface current of the North Atlantic Ocean that also constitutes a key branch of the thermohaline circulation, supplying boreal basins with warm and salty waters (Broecker et al., 1990).

2.2. Sedimentary mechanisms for the origin of the laminations

During glacial maxima, the 'Fleuve Manche' paleoriver was connected to the open ocean in the Bay of Biscay *via* submarine canyons on the continental shelf which channelled turbidite material towards two mid-sized deep sea fans, the Celtic and the Armorican turbidite systems (Auffret et al., 2000; Zaragosi et al., 2001; Toucanne et al., 2008). Many studies deal with the 'Fleuve Manche' paleoriver discharges associated with European ice sheets collapse, and the Bay of Biscay is considered as a depocentre for European erosional products (Zaragosi et al., 2001, 2006; Mojtahid et al., 2005; Eynaud et al., 2007; Toucanne et al., 2008, 2009). Core MD03-2692 is not affected by turbidites but registered hemipelagic sedimentation. However, increasing concentrations of large detrital grains (> 150 µm) reveals several events of ice-rafting during glacial periods (MIS 2 and MIS 6). Previous studies in the area (e.g. Zaragosi et al., 2001) have already demonstrated that coarse lithic grains are primarily supplied by ice-rafting and not by turbiditic processes.
Associated with coarse detrital grains, a peculiar facies of laminations was evidenced by Mojtahid et al. (2005) at the end of MIS 2 and within mid-MIS 6. The laminated facies is characterized by light and dark couplets on X-ray imagery. Millimetre to centimetre-scale layers of ungraded mud layers (bright laminae) alternate with millimetre-scale layers of IRD-rich mud (dark laminae) (Zaragosi et al., 2001; Mojtahid et al., 2005). The absence of cross bedding, graded bedding and the mainly clayey composition of all the laminae exclude a contouritic or turbiditic origin for the laminae (cf. Eynaud et al., 2007).
Eynaud et al. (2007) asked the question of laminae frequency (multiannual, annual, or seasonal). According to a seasonal decay assumption, the counting of the laminae (a couplet 'clear–dark' representing one year) would indicate that MIS 2 sequence records 91 years and not 800 as suggested by the age model (Eynaud et al., 2007). However, continuous fine laminae deposition through time is rare, even in lakes (Tian et al., 2005), and should therefore not be expected in deep-sea environments of the Bay of Biscay. Almost 200 laminae were counted during mid-MIS 6 laminated episode and we expect that this event could represent around 1000-2000 years by analogy with MIS 2. Extremely important sedimentation rates (around 500 cm/ka at the end of MIS 2) characterize the laminated periods. Therefore, laminae were firstly interpreted as constituting annual or semi-annual changes in sedimentation, considering a scenario of seasonal British Irish Ice Sheet (BIIS) decay during springtime (cf. Mojtahid et al., 2005, for further details about the conceptual model). More recently, Toucanne et al. (2009) suggested a mechanism of periodic expulsion of anchor-ice (Reimnitz and Kempama, 1987; Kempama et al., 2001) and of sediment-rich frazil ice (Reimnitz and Kempama, 1987) formed in the 'Fleuve Manche' paleoriver system during winter, when the activity of the river was low, and released during springtime in response to the increased runoff of the surrounding ice sheets and glaciers (see Toucanne et al., 2009, for further details).

3. Materials and methods

3.1. Stratigraphy of core MD03-2692

The stratigraphical framework of core MD03-2692 is based, for the first 20 ka of the record, on 12 AMS radiocarbon dates derived from monospecific samples of the planktonic foraminifera species *G. bulloides* or *N. pachyderma* s. include six dates within the laminated sequence, at the end of MIS 2 (cf. Eynaud et al., 2007, for a complete description of the methodology). In this study, we have delimited Heinrich event 1 (HE 1) by the extent of the cold event as revealed by a clear plateau of nearly 100% of the polar foraminifera *Neogloboquadrina pachyderma* s., marking at that time a southward migration of the Polar Front and cold SST in the Bay of Biscay (Pujol et al., 1973; Pujol, 1980; Pujol et al., 2000). These limits for HE 1 coincide with the radiocarbon ages given by Elliot et al. (1998, 2001) and Bard et al. (2000), between 18.3 and 15.9 ka cal B.P. (15.1 and 13.4 ka ^{14}C B.P.).
Thereafter, and up to MIS 10, we used the age model established by Toucanne et al. (2009), slightly modified from Mojtahid et al. (2005), as it provides a better constraint on mid-MIS 6 chronology which is of particular interest in the present study. Indeed, the benthic δ^{18}O composite record obtained in core MD03-2692 (by using benthic foraminifera species *Uvigerina peregrina*, *Pullenia bulloides* and *Planulina wuellerstorfi*; Mojtahid et al., 2005) shows a lag between 2,380 and 2,600 cm due to the scarcity of benthic foraminifera. Toucanne et al. (2009) compared the benthic isotope record from core MD03-2692 with that of the Ocean Drilling Program Site 980, drilled off the eastern edge of the Rockall Plateau (McManus et al., 1999), and synchronised them with the LR-04 chronology proposed by Lisiecki and Raymo (2005) (cf. Toucanne et al., 2009, for details about the chronology and for the age versus depth graph with marker points). MIS 6 boundaries were positioned according the LR-04 chronology between 130 and 191 ka B.P. Concerning mid-MIS 6, we can not know the precise duration of laminated deposits because of the lack of benthic foraminifera for isotopic analysis during this specific interval. By analogy with the laminae found at the end of MIS 2, we can assume that the scarcity of benthic foraminifera may result from a dilution due to extremely high sedimentation rates, or may also be due to an extreme weakening of the deep/intermediate water production reducing the ventilation at the bottom (Peck et al., 2006). The stratigraphical framework of the core locates the laminated event around 150 ka B.P. The observation of laminae in core MD01-2461 (Eynaud et al., 2007), retrieved from the Western Porcupine Bight (51.75°N, 12.55°W, 1153 m water depth; Fig. 1), validates this age. Indeed, the dating by U-Th methods (GEOTOP, http://www.geotop.uqam.ca/) of a perfectly preserved coral, found 200 cm above the uppermost occurrence of laminae during MIS 6, has given a date of 139.77 ka B.P. ± 2500 years (C. Hillaire-Marcel and B. Ghaled, personal communication, 2003). It implies therefore that mid-MIS 6 laminated deposits occurred prior to 140 ka B.P.
Isotope analysis, conducted on the three benthic foraminifera used to establish the benthic δ^{18}O composite record, allowed us to construct a composite benthic δ^{13}C record (cf. Penaud et al., 2008) evidencing also clearly the stratigraphy of the core through the reconstruction of the deep water paleocirculation (Duplessy and Shackleton, 1985; Raymo et al., 1990; Vidal et al., 1997).

3.2. Palynomorph analysis

3.2.1. Quaternary dinoflagellate cysts

Dinocysts were extracted from the < 150 µm sedimentary fraction. Samples were taken every 10 cm in the core. 153 slides were analysed from MIS 7 to MIS 5, between 3,220 and 1,700 cm, and 29 slides document the transition from the end of the Last Glacial Maximum to the Holocene, between 400 and 60 cm. The preparation technique followed the procedure described by de Vernal et al. (1999), slightly modified at the *UMR 5805-EPOC, Bordeaux I University* (see Penaud et al., 2008). For each sample, an average of 300 specimens were identified and counted using a Leica DM 6 000 microscope at 400 × magnification, except for the two laminated episodes between 2,576 and 2,424 cm (mid-MIS 6) and between 295 and 186 cm (MIS 2 termination) for which an average of 30 and 60 specimens per slide was respectively obtained. In order to estimate palynomorph concentrations on volume of dried sediment, aliquot volumes of *Lycopodium* spores were added to each sample before chemical treatments (marker grain method; de Vernal et al., 1999). Taxonomic identifications conform to the ones of Fensome et al. (1998) and Fensome and Williams (2004), and *Brigantedinium* cysts are grouped and include all spherical brown cysts as it is difficult to identify them to species level. Dinocysts assemblages are described with the relative abundances of each species calculated on the basis of the total sum of dinocysts including unidentified taxa and excluding pre-Quaternary cysts.

3.2.2. Reworked tracers

Other palynomorphs were systematically counted separately on each slide. Pre-Quaternary cyst concentrations and the ratio Reworked (pre-Quaternary) versus Modern dinocysts (Rd/Md) allowed determination of periods with allochtonous sedimentary supply (Spiegler, 1989), as previously demonstrated in the Bay of Biscay (Eynaud, 1999; Kaiser, 2001; Zaragosi et al., 2001). Kaiser (2001, unpublished data) worked on several slides from laminated intervals of core MD95-2002 in order to qualitatively study pre-Quaternary cysts and infer geological sources for the terrigenous inputs occurring in the Bay of Biscay. This study has revealed a biostratigraphic distribution of reworked cysts from the second half of the Mesozoic (late Jurassic) to the early Tertiary (Miocene). Specific sources were not identified since most of NW European geological formations are that age. However, the 'Fleuve Manche' paleoriver substratum may have been a source of pre-Quaternary dinocysts as it is formed by early Jurassic to early Tertiary geological formations (Kaiser, 2001; Gupta et al., 2007). Lands drained by the paleoriver tributaries are also potential sources.
Coenobia of the freshwater micro-algae *Pediastrum* spp. were also counted on the same slides. The occurrence of *Pediastrum* spp. coenobia in marine environments is related to fluvial discharges (Lézine et al., 2005) towards the open ocean, as also previously observed in the Bay of Biscay (Zaragosi et al., 2001; Ménot et al., 2006).

4. Results from core MD03-2692

4.1. MIS 2 - Termination I

The termination of the LGM sequence shows high relative abundances of the species *Operculodinium centrocarpum* (Fig. 2a), considered to be a tracer of the North Atlantic Drift (NAD) since its present-day distribution in surface sediments of the North Atlantic follows the superficial branch of the thermohaline circulation and especially the NAD (Turon, 1984; Rochon et al., 1999; Eynaud et al., 2004; Penaud et al, 2008). The percentages of this species, up to 80% of the total dinocysts assemblages, are consistent at that time with low relative abundances of the polar foraminifera *Neogloboquadrina pachyderma* s. (Fig. 2a). The latter, whose percentages do not exceed 20% of the planktonic foraminifera assemblage at the end of the LGM, reflects subpolar conditions similar to the one recorded today North of the NAD where the same relative abundances are reached within surface sediments. At the end of the LGM, high *Pediastrum* spp. coenobia concentrations are observed as well as the presence of reworked dinocysts (Fig. 2a). *Pediastrum* spp. coenobia concentrations decrease then just before Heinrich Event 1 (HE 1; Fig. 2a).

In the North Atlantic Ocean, Heinrich events are recognized usually on the basis of the presence of ice rafted detritus (IRD), high polar foraminifera (*N. pachyderma* s.) relative abundances and heavy planktonic $\delta^{18}O$ values (e.g. Heinrich, 1988; Bond et al., 1993; Grousset et al., 1993; Bond and Lotti, 1995; Lebreiro et al., 1996; Bard et al., 2000; de Abreu et al., 2003; Hemming, 2004). The beginning of HE 1 in our record (Fig. 2a) is characterized by the strong decline of *Operculodinium centrocarpum*. HE 1 is then identifiable by nearly 100% of the polar foraminifera *N. pachyderma* s. and very low Quaternary dinocyst concentrations reflecting a very low primary productivity or a dilution by terrigenous material (Fig. 2a). Based on the occurrence of laminae, HE 1 can be divided into two distinct phases, a laminated interval that we have called HE 1a, and a second phase without laminae that we have called HE 1b (Fig. 2a). Synchronous with the appearance of the unusual laminated facies, a substantial rise in the ratio [Rd/Md] and in *Pediastrum* spp. coenobia concentrations is observed (Fig. 2a), and very few Quaternary dinocysts were counted (average of only 60 specimens per slide). Therefore, interpretation based on Quaternary dinocysts assemblages during this interval must be considered with caution and we decided to downplay their significance (Table 1; cf. “quasi-barren samples” on Fig. 2a).

At the end of HE 1a, the sudden and drastic drop in laminae is accompanied by a strong decline of reworked tracer concentrations (Fig. 2a). During HE 1b, coarse lithic grain concentrations increase by a factor 4 to 5 in comparison with the laminated interval, reaching 2,000 grains/g. of dry sediments (Fig. 2a). Two major occurrences of the subpolar dinocyst *Bitectatodinium tepikiense* (Fig. 2a) are observed, corresponding with two major peaks of coarse detrital material. *B. tepikiense* has also been observed previously during HE 1 in the Mediterranean Sea (Combourieu-Nebout et al., 2002) and off the Iberian margin (Eynaud, 1999; Turon et al., 2003). This taxon, abundant in present-day dinocysts assemblages north of 53°N in North-western Atlantic sediments, with a maximum occurrence at the mouth of the Gulf of St. Lawrence, tolerates large seasonal amplitudes of temperatures and a wide range of salinities (Rochon et al., 1999). A brief incursion of the respectively subpolar and polar taxa *Spiniferites elongatus* and *Islandinium minutum* (Rochon et al. 1999) can also be noted, even if they do not represent a significant part of the assemblage (Fig. 2a).

HE 1 is followed by the Bölling/Allerod (B/A) mainly characterized, in our sequence, by increasing percentages of *Nematosphaeropsis labyrinthus*. *N. labyrinthus* is abundant in cool areas, between 45 and 65°N in the North Atlantic (Marret et al., 2004; de Vernal et al., 2005). During this relatively warm interval, *N. pachyderma* s. percentages decrease strongly and the warm set of *Impagidinium* spp. develops (Fig. 2a).

The succeeding Younger Dryas (YD) is marked by a strong decline of *N. labyrinthus*, an increase in cysts of *Pentapharsodinium dalei*, and high percentages of the polar foraminifera *N. pachyderma* s. Cysts of *P. dalei* are well represented in modern sediments from polar to subpolar environments that experience sea-surface summer temperatures higher than 4°C (Rochon et al., 1999; Matthiessen, 1995; Marret et al., 2004; de Vernal et al., 2005).

4.2. MIS 6 – Termination II

Figure 2b presents our data over a period including MIS 7, MIS 6 and MIS 5. The warm set of species composed of *Spiniferites mirabilis* and *Impagidinium* spp., abundant today in warm to temperate domains (Turon, 1984; Rochon et al., 1999), shows clearly the two Interglacial Complexes (MIS 5 and MIS 7), while the central part of the diagram describes the penultimate glacial stage (MIS 6). For a detailed study of MIS 5 and MIS 7 paleoenvironmental history in the Bay of Biscay, we refer to Penaud et al. (2008). Recurrent successions of species both at the beginning and at the termination of the Interglacial Complexes were noted by these authors, with the temporal succession of *Operculodinium centrocarpum*, *Nematosphaeropsis labyrinthus* and cysts of *Pentapharsodinium dalei*, from an interglacial period to a glacial one; and the succession of *N. labyrinthus* followed by *O. centrocarpum*, the latter marking the onset of the Interglacial Complexes, when the climate switched from glacial to interglacial conditions. Glacial conditions are indicated by the strong development of cysts of *P. dalei* (Fig. 2b) at the onset of MIS 6. Within the penultimate glacial stage cold taxa developed significantly include *Bitectatodinium tepikiense*, cysts of *Pentapharsodinium dalei* (cf. Marret et al., 2004; de Vernal et al., 2005, for the actual distribution of these taxa), and *Spiniferites septentrionalis* (Penaud et al., 2008).

Within mid-MIS 6, as in HE 1, an extremely important cold interval centred around 2,500 cm is deduced from a plateau of high abundances of the polar foraminifera *N. pachyderma* s., synchronous with increasing concentrations of coarse detrital material and extremely low Quaternary dinocyst concentrations (Fig. 2b). This cold event can be divided into two distinct parts, the first one displaying very high concentrations of laminae (Fig. 2b). However, the laminated facies is not restricted to the interval described above and appears as early as 2,780 cm depth in the core (Fig. 2b). For this reason, we have differentiated the two laminated phases referring to “Phase 1” (2,780 cm - 2,580 cm), and “Phase 2” (2,580 - 2,420 cm). “Phase 1” laminated event is coeval with a small increase of *Pediastrum* spp. coenobia and pre-Quaternary cyst concentrations, while “Phase 2” is coeval with very strong concentrations of these reworked tracers (Fig. 2b).

5. Discussion

5.1. The primary productivity pattern of MIS 6

Figure 3 depicts a multiproxy compilation which shows the distinction between colder and warmer intervals through MIS 6. During warmer periods, Quaternary dinocyst concentrations are very high (20,000 to 50,000 cysts/cm^3) and *Neogloboquadrina pachyderma* s. percentages are extremely low. This may be linked to a high primary productivity related to high SST, as also suggested synchronously by higher planktonic foraminifera concentrations and higher values of Ca-XRF. The calcium is considered as mainly originating from biogenic $CaCO_3$ since this parameter has been previously observed as co-varying with strontium data and absolute abundances of foraminifera (Mojtahid et al., 2005). The measurement of major elements in core MD03-2692 has been undertaken by CORTEX X-ray-fluorescence (XRF), using the ‘Avaatech core-scanning XRF’ of the University of Bremen, at 2 cm resolution (Mojtahid et al., 2005). *Brigantedinium* spp. concentrations are also shown on Figure 3. These species are a good indicator of regions influenced by high productivity such as those influenced by seasonal upwelling (e.g. Marret, 1994; Zonneveld et al., 2001; Radi and de Vernal, 2004). Indeed, the occurrence of *Brigantedinium* spp. is more often the result of prey availability, including diatoms. It supports indirectly the interpretation of higher primary productivity resulting from higher nutrient concentrations in the water column. In addition, it is worth noting that *Brigantedinium* spp. concentrations follow the general trend of Quaternary dinocyst concentrations.

By contrast, during colder intervals, very low Quaternary dinocyst concentrations (500 to 5,000 cysts/cm^3) reflect low primary productivity, and high *N. pachyderma* s. abundances are observed. Cold events are also systematically found coeval with a high content of coarse detrital material and high inputs of terrigenous elements illustrated by the ratio: sum (counts/second) of XRF-derived terrigenous elements (Titane: Ti and Iron: Fe) versus sum of XRF-derived biogenic elements (Calcium: Ca and Strontium: Sr). Toucanne et al. (2009) used the ratio of XRF intensities Ti/Ca to estimate terrigenous inputs from the ‘Fleuve Manche’ paleoriver at MD03-2692 site.

Although foraminifera and dinocysts are two marine proxies with very different ecological affinities and requirements, as well as different chemical compositions of their walls, we observed an unambiguous anti-correlated signal between *N. pachyderma* s. relative abundances and Quaternary dinocyst concentrations throughout MIS 6. This observation is consistent with results from Rasmussen et al. (2002). They studied benthic and planktonic foraminifera on North Atlantic cores during the last glacial period and found a lower productivity signal during stadials and Heinrich events. Our data reveal that the Quaternary dinocyst community, representing a significant part of the global phytoplanktonic community, shows also a clear pattern of paleoproductivity during MIS 6. Schmittner (2005) recently studied the consequences of disturbances of the thermohaline circulation on the marine ecosystem, injecting freshwater in the North Atlantic in a coupled climate-ecosystem model of intermediate complexity. Simulations show that a disruption of the thermohaline circulation leads to a collapse of the plankton stocks. The response is most dramatic in the North Atlantic and is caused by the decrease of upper ocean nutrient concentrations (Schmittner, 2005). We can assume that a weakening of the deep water formation occurred during MIS 6 cold events as it was the case during the Heinrich events of the last glacial cycle (Vidal et al., 1997). Our data would be then in accordance with such modelling, showing that the global ocean productivity (zoo- and phytoplankton) is sensitive to changes in the Atlantic Meridional Overturning Circulation.

5.2. MIS 2/Termination I: A scenario for the last European deglaciation based on cores MD03-2692 and MD95-2002

5.2.1. The end of the Last Glacial Maximum

The end of the Last Glacial Maximum (LGM) is characterized by the presence of high relative abundances of the dinocyst species *Operculodinium centrocarpum* (Fig. 4), considered to be a tracer of the NAD. The presence of the NAD in the Bay of Biscay, during the last part of the LGM, is also coherent with GCM model results which have shown a shift of the NADW convective centres during this period towards temperate latitudes (Cottet-Puinel et al., 2004), with then deep convection occurring only in a small area off the western coast of Europe, namely the Bay of Biscay. We reinforce here the idea that the LGM interval can be interpreted, in the North Atlantic, as a “warm” SST episode in comparison with the surrounding cold Heinrich events (HE 2 and HE 1). The LGM has long been considered as a period of extremely cold sea-surface conditions as far as 40°S (CLIMAP Project Members, 1981). A recent re-evaluation of global SST (MARGO Project; Kucera et al., 2005), based on the international EPILOG initiative to define an accurate chrono-interval for the LGM (carefully avoiding HE 1 and HE 2; Mix et al., 2001), but also based on the new and diversified proxies available for SST reconstructions (e.g. Mg/Ca, alkenones, Quaternary dinocyst and foraminifera new transfer functions), has shown that this period is actually marked by contrasting conditions, with SST that could be as high as present-day ones in the northern Atlantic Ocean (GIN seas, Greenland-Iceland-Norwegian Seas), at least during summer (e.g. de Vernal et al., 2005, 2006).

At the end of the LGM, relatively high SST were previously suggested in the same area as a trigger for BIIS instability during HE 1 (Zaragosi et al., 2001; Mojtahid et al., 2005; Peck et al., 2006). Since the NAD is today responsible for mild and moderate climatic conditions over the Western European region, two hypotheses have been formulated previously to explain European ice sheets destabilization. Firstly, the northward penetration of low latitude warm and saline waters from the NAD brought humidity into northern latitudes. The collapse of European ice sheets may then derive from an increase of precipitation amplifying in return the ice accumulation and reducing ice sheets stability, according to the binge/purge model of Alley and MacAyeal (1994). Secondly, the instability of BIIS shelves may have been induced by warmer SST (Moros et al., 2002; Hulbe et al., 2004). Indeed, Ballantyne et al. (2008) calculated the projected minimum offshore extent of the BIIS during the LGM, implying that the ice sheet expanded 25 km offshore towards western Ireland. However, it seems that both concepts (sea-level rise due to iceberg calving and subsurface ocean warming) must be combined to obtain a credible scenario for European ice sheets destabilization, as it was demonstrated by simulations of abrupt glacial climate changes (Flückiger et al., 2006).

At the end of the LGM, high concentrations of freshwater algae *Pediastrum* spp. coenobia are observed in core MD03-2692 around 18.2 ka cal B.P. (Fig. 4a), as well as in core MD95-2002 around 20 ka cal B.P. (Zaragosi et al., 2001). An increase of the BIT (Branched and Isoprenoid Tetraether) index (core MD95-2002; Ménot et al., 2006), as well as enhanced seaward sediment transfer on the Celtic - Armorican margin (Toucanne et al., 2008, 2009), were also previously observed at that time. Therefore, increasing continental supplies and fluvial discharges *via* the 'Fleuve Manche' paleoriver system, caused by the gradual retreat of European ice sheets and glaciers, occurred at the end of the LGM in response to the last deglaciation inception and to the rise in insolation at 65°N. The following abrupt sea-level rise may have prevented seaward transfer of material by the 'Fleuve Manche' paleoriver around 18 ka cal B.P., just before HE 1, as revealed synchronously by the decrease of *Pediastrum* spp. coenobia concentrations (Fig. 4), the episodic decrease of the frequency of turbidite deposits in the Armorican system (Toucanne et al., 2008), and the decrease of the BIT-index (Ménot et al., 2006).

5.2.2. Heinrich event 1 (HE 1a and HE 1b)

Ice-rafting that occurred during HE 1 (from 15 to 18 ka cal B.P., Fig. 4) leads to a cold event which might have disrupted the convective overturning (Broecker et al., 1990). The decline of the NAD is interpreted in our results through the strong decrease in *O. centrocarpum* percentages. The BIIS is situated close to the main Atlantic convective centres and this context enhances the potential of freshwater inputs to perturb the AMOC as was demonstrated in the Porcupine Sea Bight, proximal to the BIIS, by a sharp decrease of the benthic $\delta^{13}C$ values during periods of BIIS instability (Peck et al., 2006).

First phase of HE 1: laminated interval (HE 1a)

A substantial rise in the ratio [Rd/Md] and in *Pediastrum* spp. coenobia concentrations are observed around 18 ka cal B.P., in cores MD03-2692 and MD95-2002 (Fig. 4), synchronous with the appearance of the laminated facies. This facies is also characterized by high terrigenous supply frequency in the Celtic and Armorican turbidite systems (Toucanne et al., 2008, 2009), and maximal values of the BIT-index (core MD95-2002; Ménot et al., 2006). Indeed, 'Fleuve Manche' paleoriver discharges increased significantly in response to the seasonal influx of meltwater associated with the retreat of European ice sheets and glaciers, especially during springtime (Mojtahid et al., 2005; Toucanne et al., 2009). The fluvial discharges induced the erosion of old geological European provinces, as well as the erosion of the substratum of the 'Fleuve Manche' paleoriver itself (Gupta et al., 2007), resulting in the presence of reworked dinocysts in the open ocean.

It has been previously shown that the arrival of Canadian derived material along the European margin (also referred to Heinrich layers in the North Atlantic, and more precisely in the Ruddiman belt between 40 and 55°N; Ruddiman, 1977) is preceded by European IRD (e.g.

sedimentological data, lithological identification, Sr and Nd isotopic composition; Snoeckx et al., 1999; Grousset et al., 2000; Scourse et al., 2000; Zaragosi et al., 2001; Peck et al., 2007). Therefore, the early instability of European ice sheets has been suggested to have played a mechanistic role in the initiation of the Laurentide Ice Sheet (LIS) collapse. Here, we reinforce the idea that the mixed signal of massive clays associated with laminae rich in European fluvial coarse detrital material (from 18 to 17 ka cal B.P.) is not a precursor for HE 1 in the North-eastern Atlantic, as suggested by many publications (e.g. Snoeckx et al., 1999; Grousset et al., 2000; Zaragosi et al., 2001; Ménot et al., 2006; Peck et al., 2007), but is integrated within HE 1 and constitutes its first part.

Second phase of HE 1: cold and dry interval (HE 1b)

The simultaneous sudden and drastic drop of laminae and reworked tracer concentrations (*Pediastrum* spp. coenobia and pre-Quaternary cysts), around 17 ka cal B.P. (Fig. 4), indicates a substantial decrease of the ‘Fleuve Manche’ paleoriver runoff. Synchronously, a decrease in mass accumulation rates (Toucanne et al., 2009) and of turbiditic activity in the Celtic-Armorican turbidite systems (Toucanne et al., 2008), suggests also a different mechanism of sedimentation on the Celtic-Armorican margin with less inputs of terrigenous material.
During HE 1b, a brief incursion of the taxon *Islandinium minutum*, as well as major occurrences of the subpolar dinocyst *Bitectatodinium tepikiense* clearly associated with major peaks of coarse detrital material (Fig. 4), indicate drastic sea-surface conditions, and probably the development of a seasonal sea-ice cover along the continental borders of the Bay of Biscay. Polar conditions prevailing over NW Europe were also previously observed (Zaragosi et al., 2001; Mojtahid et al., 2005; Peck et al., 2007). Moreover, a peak of magnetic susceptibility typical of the Laurentide signature (Grousset et al., 2000) is noted in cores MD95-2002 (Zaragosi et al., 2001) and MD03-2692 (Mojtahid et al., 2005), and research on IRD on the basis of the $\varepsilon_{Nd}(0)$ have permitted discrimination of Canadian versus European IRD sources (Grousset et al., 2000). The second part of HE 1 corresponds then to the major calving of pan-Atlantic ice sheets (Zaragosi et al., 2001; Mojtahid et al., 2005), including massive iceberg discharges from the Laurentide Ice Sheet (Grousset et al., 2000; Zaragosi et al., 2001), documented as early as 17.5 ka cal B.P. in the North Atlantic by a cessation of the AMOC (McManus et al., 2004). The strong weakening of production of deep waters in the North Atlantic is contemporaneous with the general re-advance phases of the BIIS (McCabe et al., 2007), the Fennoscandian Ice Sheet, and European glaciers (Buoncristiani and Campy, 2004; Everest et al., 2006; Ivy-Ochs et al., 2006; Knies et al., 2007). At that time, the inactive NAD may have prevented the melting of European ice sheets permitting them to expand in a context of extremely cold climate.

5.3. MIS 6/Termination II: towards a better understanding of the hypothetical forcing acting on European glaciated systems

The cold event centred on 150 ka B.P. can be divided into two parts, as in HE 1, with laminated deposits recorded in the earlier phase only (Fig. 5). Contrary to MIS 2 laminae associated with Termination I, this strong concentration of laminae within mid-MIS 6 appears 20 ka earlier than Termination II (Fig. 5). Previous studies have suggested that the laminated event identified within mid-MIS 6 may be linked to an early BIIS collapse induced by low-latitude climatic changes (Mojtahid et al., 2005; Eynaud et al., 2007). This hypothesis was supported by the observation of a rise in the low latitude insolation at 15°N around 150 ka B.P. (Fig. 5), and also by previous studies on equatorial cores reporting an early warming before the onset of the northern hemisphere penultimate deglaciation (Schneider et al., 1999; Lea et al., 2002). Here, we investigate in detail the chronology of the paleoclimatological changes affecting the whole MIS 6 in order to better constrain the early decay of European ice sheets in the broader frame of the penultimate glacial history.

5.3.1. Initiation of the penultimate glacial period

The onset of MIS 6 is marked by a clear drop of benthic oxygen values (Fig. 5). Benthic oxygen isotopes usually permit assessment of the ice volume covering northern hemisphere latitudes and thus deduction of the amplitude of sea-level changes (e.g. Waelbroeck et al., 2002). The composite relative sea-level (RSL) curve of Waelbroeck et al. (2002), based on robust regressions applied to long benthic foraminifera oxygen isotopic records from the North Atlantic and the Equatorial Pacific Ocean, indicates an order of magnitude of sea-level changes within MIS 6 (Fig. 5). Therefore, we can see that sea-level is decreasing as a consequence of the formation of polar ice-caps in the northern hemisphere at the beginning of MIS 6. No important ice-rafting occurred at that time in the Bay of Biscay and this build-up without iceberg calving lasted around 5-6 ka until the beginning of MIS 6.5 event (Fig. 5).

5.3.2. MIS 6.5: “interglacial” conditions within a glacial period

MIS 6.5 is known to record unusual warm conditions for a glacial period, close to interglacial ones (e.g. Rossignol-Strick, 1983; Malaizé et al., 1999, Masson et al., 2000; Bard et al., 2002). A strong environmental change around 175 ka B.P. during MIS 6.5 has been detected in ice-core records through an anomaly in the so-called Dole effect (Malaizé et al., 1999). Studies conducted on each side of the equatorial African continent, on the Socotra Basin (Indian Ocean) (Malaizé et al., 2006) and on the Mauritanian margin (Tisserand et al., in press), suggested a northward shift of the ITCZ getting closer to mid-latitudes between 180 and 165 ka B.P. Furthermore, a strong monsoon index was calculated by Rossignol-Strick (1983; Fig. 5), an unusual sapropel event (S6) for glacial conditions occurred in the eastern Mediterranean Sea (Cheddadi and Rossignol-Strick, 1995; Fig. 5), and strong Mediterranean rainfalls were registered by stalagmite $\delta^{18}O$ records (Argentarola Cave, Bard et al., 2002; Soreq Cave, Ayalon et al., 2002; Fig. 5). Masson et al. (2000), who simulated this event for the first time, concluded that strong insolation can generate an increase in monsoon activities even during glacial times, and demonstrated that increasing North Atlantic and Pacific surface winds during MIS 6.5 can affect bioproductivity. Our results reveal furthermore that this warm and humid period was actually marked by relatively high Quaternary dinocyst concentrations (Fig. 5), probably reflecting warmer conditions and higher productivity in the Bay of Biscay. Furthermore, typical interglacial vegetation has been observed in Northern Iberia around 175 ka B.P. (Leymarie, 2008, unpublished data from core MD01-2447).

5.3.3. The laminated events within MIS 6

Comparison “Phase 1” (160-170 ka B.P.) – “Phase 2” (around 150 ka B.P.)

Immediately following MIS 6.5, the primary productivity, as inferred from Quaternary dinocyst concentrations, decreases abruptly and the first laminae are recorded (Fig. 5). The laminae, between 160 and 170 ka B.P., show a two-step pattern consistent with two peaks of *N. pachyderma* s. relative abundances, increases of coarse lithic grain concentrations, and slight increases of *Pediastrum* spp. coenobia and pre-Quaternary cyst concentrations (Fig. 5). During MIS 6.5, the increase in relative humidity in mid-latitudes through higher precipitation (e.g. Bard et al., 2002; Ayalon et al., 2002) may have contributed to the growth of European ice sheets. These may have reached a threshold leading to their first partial collapse and then to intensification of ‘Fleuve Manche’ paleoriver discharges.

This first partial collapse of European ice sheets was probably not as pronounced as the second one occurring around 150 ka B.P. in phase with an increase in northern hemisphere summer insolation, though less important than the insolation maxima recorded during MIS 6.5 and Termination II (Fig. 5). This laminated event is synchronous with very strong occurrences of reworked tracers showing an episode of extreme fluvial discharges *via* the ‘Fleuve Manche’ paleoriver (Fig. 5). High terrigenous supply is also revealed at that time through very important mass accumulation rates (Toucanne et al., 2009), with values probably comparable at least with those observed at the end of the last glacial period during HE 1a (155 g/cm²/ ka). It is interesting to note that the signal of Soreq Cave shows minimum $\delta^{18}O$ values at 178 and 152 ka B.P. (Ayalon et al., 2002), that is to say before “Phase 1” and “Phase 2” respectively. Atmospheric conditions in the Mediterranean basin were then relatively humid associated with wet tropics, and with a high monsoon index related to precession minima and insolation maxima (Fig. 5; Ayalon et al., 2002). Weldeab et al. (2003), working on several sequences from the Eastern and Western Mediterranean Sea with barium contents to reconstruct changes in sea-surface productivity during times of sapropel formation, have detected an interval of elevated productivity around 150 ka B.P. in phase with the summer insolation maximum at 65°N. They have concluded that the northern hemisphere insolation peak at 150 ka B.P. was insufficient to trigger a sapropel formation; however, it was strong enough to induce productivity changes six times higher than during deposition of the surrounding sediments in between sapropels 5 and 7 in the Mediterranean Sea. Several paleo sea-level records show a high global sea-level around 140-135 ka B.P. (e.g. Winograd et al., 1992, 1997; Ludwig et al., 1992; Esat et al., 1999; Henderson and Slowey, 2000; Gallup et al., 2002) that could be the consequence of the early significant but partial melting of European ice sheets 20 ka earlier than Termination II. During the period of increasing ‘Fleuve Manche paleoriver’ discharges, Toucanne et al. (2009) observed also a lightening of benthic $\delta^{18}0$ values of about 0.55 ‰ in ODP Site 980 (Rockall Plateau), that may represent a global rise of sea-level of about 15-20 m according to Waelbroeck et al. (2002). Moreover, if we take a look at the composite RSL curve (Fig. 5), we can notice a low but significant sea-level rise following “Phase 2” laminated episode that may result from the partial collapse of European glaciated systems.

According to our benthic oxygen values and to the composite RSL curve of Waelbroeck et al. (2002; Fig. 5), it is obvious that sea-level was higher during “Phase 1” than during “Phase 2”. Therefore, we can assume that the BIIS was not connected to the Fennoscandian Ice Sheet during “Phase 1”, but that this connection was established during “Phase 2” when sea-level was lower (Fig. 5). Meltwater from European lowlands could then have been canalized only *via* the ‘Fleuve-Manche’ paleoriver in the Bay of Biscay during “Phase 2”, resulting in stronger concentrations of laminae and reworked tracers. This theory is reinforced by Toucanne et al. (2009) who have depicted a schematic paleogeographical configuration of Western Europe throughout the penultimate glaciation.

Comparison “Phase 2” (around 150 ka B.P.) - HE 1a (around 18 - 17 ka cal B.P.)

“Phase 2” laminated interval is very similar to the laminated deposits observed at the beginning of Heinrich event 1 (HE 1a) in terms of paleohydrological changes. However, the strength of the fluvial discharges during mid-MIS 6 was probably much higher than during MIS 2 termination. This assumption is based on a comparison of Quaternary dinocysts and allochtonous tracer (*Pediastrum* spp. coenobia and pre-Quaternary dinocyst) concentrations between mid-MIS 6 and HE 1a (Table 1). This may be due to the extent of European ice sheets during the penultimate Glacial Complex MIS 6 (see Fig. 1 for the extent of the BIIS during MIS 2 and MIS 6 after Svendsen et al., 2004 and Ehlers and Gibbard, 2004). Toucanne et al. (2009) have correlated MIS 6 with the extensive Saalian glaciations, and Svendsen et al. (2004) showed that during the Late Saalian (160-140 ka B.P.), one of the most extensive glaciations of the last 160 ka, a huge ice sheet complex was probably formed over northern Eurasia. We can assume that a southward extension of European ice sheets occurred during MIS 6, even if there is no evidence (cf. Fig. 1). It could then explain the stronger sensitivity of southern European ice sheets margins to climate change around 150 ka B.P.

5.3.4. The end of MIS 6: 140 to 130 ka B.P.

Finally, the latest part of the record after 140 ka B.P. shows very high values of benthic oxygen isotopes (around 4.7‰; Fig. 5) indicating a very low sea-level, as confirmed by Waelbroeck et al. (2002; Fig 5). Species such as *Bitectatodinium tepikiense* and *Nematophaeropsis labyrinthus,* marking cold periods in the Bay of Biscay (Penaud et al., 2008), are recorded (Fig. 2b). Considering the benthic carbon isotopic signal, very light values suggest a strong weakening of the ventilation (Fig. 5). This fact is even more obvious when comparing the later part of the record between 130 and 141 ka B.P. (mean value of -0.28 ‰) with the heavier values recorded in the first part of MIS 6 between 170 and 190 ka B.P. (mean value of -0.07 ‰). It demonstrates a lower ventilation of the deep ocean at the end of MIS 6.

5.3.5. Termination II

Unlike Termination I, no laminae are recorded at the onset of Termination II in the Bay of Biscay (Fig. 5). However, the substantial retreat of European ice sheets occurring around 150 ka B.P. was probably partial. Indeed, the transition between the end of MIS 6 and the start of the last Interglacial Complex is marked by an important decrease of about 2 ‰ in the benthic $\delta^{18}O$ curve (Fig. 5), imprint of the huge melting of pan-Atlantic ice sheets at the end of the penultimate Glacial Complex inducing MIS 5 high sea-level (Waelbroeck et al., 2002; Fig. 5). Toucanne et al. (2009) suggest that the non-occurrence of laminae during Termination II may be linked with the paleogeographical pattern of Western Europe and ice-free conditions between the British Isles and the Scandinavia after the huge melting event around 150 ka B.P. Therefore, during Termination II, European meltwaters were probably able to flow *via* the Manche and through the North Sea basin. This configuration would then have decreased the strength of 'Fleuve Manche' paleoriver discharges diluting the melting signal between several different basins.

Conclusions

Our results show that *Pediastrum* spp. coenobia and pre-Quaternary dinocyst concentrations present maximal values during laminated deposits found in the Bay of Biscay at the end of MIS 2 and within mid-MIS 6. It results from a huge advection of ice-rafting, fluvial waters, and sediments, from the proximal continent towards the Bay of Biscay *via* the 'Fleuve Manche' paleoriver, in response to the seasonal melting of European glaciated systems. Although both laminated events are very similar, mid-MIS 6 episode is, however, more intense in terms of 'Fleuve Manche' paleoriver discharges than those occurring at the end of MIS 2. We illustrate here the fact that each deglaciation, more precisely here Termination I and II, responds to a distinctive deglaciation pattern.

During the MIS 2 laminated episode, seasonal melting events of European ice sheets are the consequence of a climatic warming linked to high northern hemisphere summer insolation at the onset of the last deglaciation. In addition, our new dinocyst study conducted on core MD03-2692 depicts a strong reproducibility with previous dinocysts data acquired from a proximal sequence (MD95-2002), retrieved from the Meriadzek plateau at a water depth of 2,174 m, *i.e.* 2,000 m above MD03-2692 site. The good reproducibility underlines the important preservation of dinocysts and eliminates bias due to transport of cysts. It enables validation of Quaternary dinocysts as robust tools for reconstructing paleohydrological and paleoclimatic changes.
During MIS 6, we show here that the collapse of European mid-latitudes ice sheets around 170 ka B.P. may have immediately followed MIS 6.5 warming phase, and thus may be linked to the warm and humid Mediterranean climate prevailing during the formation of sapropel 6. The second important collapse of European glaciated systems occurred around 150 ka B.P., 20 ka earlier than Termination II, and corresponded to a major event of maximal ice-rafting within mid-MIS 6. This interval is synchronous with a maximum in June insolation at 65°N, though less important than during MIS 6.5 and Termination II. Similar to the first phase of laminae (170 ka B.P.), the laminae formed around 150 ka B.P. are synchronous with an aborted sapropel in the Eastern Mediterranean. The most pronounced second phase of laminae registered in the Bay of Biscay during mid-MIS 6 may be explained by the fact that, contrary to 170 ka B.P., the BIIS and the Fennoscandian Ice Sheet were connected at 150 ka B.P., permitting meltwaters to be canalized only *via* the ‘Fleuve-Manche’ paleoriver.

Acknowledgements

Thanks to IPEV, the captain and the crew of the *Marion Dufresne* and the scientific team of the SEDICAR cruise. We wish to thank Mr. Y. Balut for his assistance at sea and M. Castera, M. Georget and O. Ther for invaluable laboratory technical assistance. We thank also the ARTEMIS Project for the precious radiocarbon dating measurements; the French Programmes “ACTION MARGES”, “RELIEFS DE LA TERRE”, and the ANR “IDEGLACE”. We gratefully acknowledge Fabienne Marret and Gareth Davies for the English revision. This is a U.M.R. / EPOC C.N.R.S. 5805 contribution.

References

Alley, R.B., MacAyeal, D.R., 1994. Ice-rafted debris associated with binge/purge oscillations of the Laurentide Ice Sheet. Paleoceanography 9 (4), 503-511.
Auffret, G., Zaragosi, S., Voisset, M., Droz, L., Loubrieu, B., Pelleau, P., Savoye, B., Bourillet, J.-F., Baltzer, A., Bourquin, S., Dennielou, B., Coutelle, A., Weber, N., Floch, G., 2000. First observations on the morphology and recent sedimentary processes of the Celtic Deep Sea Fan [Premieres observations sur la morphologie et les processus sedimentaires recents de l’Eventail celtique]. Oceanologica Acta 23 (1), 109-116.

Ayalon, A., Bar-Matthews, M., Kaufman, A., 2002. Climatic conditions during marine oxygen isotope stage 6 in the eastern Mediterranean region from the isotopic composition of speleothems of Soreq Cave, Israel. Geology 30 (4), 303-306.

Ballantyne, C.K., Stone, J.O., McCarroll, D., 2008. Dimensions and chronology of the last ice sheet in Western Ireland. Quaternary Science Reviews 27 (3-4), 185-200.

Bard, E, Rostek, F., Turon, J.-L., Gendreau, S., 2000. Hydrological Impact of Heinrich Events in the Subtropical Northeast Atlantic. Science 289 (5483), 1321-1324.

Bard, E., Delaygue, G., Rostek, F., Antonioli, F., Silenzi, S., Schrag, D.P., 2002. Hydrological conditions over the western Mediterranean basin during the deposition of the cold Sapropel 6 (ca. 175 kyr B.P.). Earth and Planetary Science Letters 202, 481-494.

Berger, A., Loutre, M.F., 1991. Insolation values for the climate of the last 10 million years. Quaternary Science Reviews 10 (4), 297-317.

Bond, G., Broecker, W., Johnsen, S., McManus, J., Labeyrie, L., Jouzel, J., Bonani, G., 1993. Correlations between climate records from North Atlantic sediments and Greenland ice. Nature 365, 143–147.

Bond, G.C., Lotti, R., 1995. Iceberg discharges into the North Atlantic on millennial time-scales during the last glaciation. Science 267, 1005–1010.

Bourillet, J.-F., Turon, J.-L., 2003. Rapport scientifique de la mission MD133/SEDICAR. OCE/2003/04. Les Rapports de Campagne à la Mer IPEV, Brest, 150 pp.

Bourillet, J.-F., Reynaud, J.-Y., Baltzer, A., Zaragosi, S., 2003. The ‘Fleuve Manche’: The submarine sedimentary features from the outer shelf to the deep-sea fans. Journal of Quaternary Science 18 (3-4), 261-282.

Broecker, W.S., Bond, G., Klas, M., 1990. A salt oscillator in the glacial Atlantic? 1. The concept. Paleoceanography 5 (4), 469-477.

Buoncristiani, J.F., Campy, M., 2004. Expansion and retreat of the Jura ice sheet (France) during the last glacial maximum. Sedimentary Geology 165 (3-4), 253-264.

Cheddadi, R., Rossignol-Strick, M., 1995. Eastern Mediterranean Quaternary paleoclimates from pollen and isotope records of marine cores in the Nile cone area. Paleoceanography 10 (2), 291-300.

CLIMAP Project Members, 1981. Seasonal reconstructions of the earth’s surface at the last glacial maximum. Geological Society of America Map and Chart Series MC-56.

Combourieu-Nebout, N., Turon, J.-L., Zahn, R., Capotondi, L., Londeix, L., Pahnke, K., 2002. Enhanced aridity and atmospheric high-pressure stability over the western Mediterranean during the North Atlantic cold events of the past 50 k.y. Geology 30 (10), 863-866.

Cottet-Puinel, M., Weaver, A.J., Hillaire-Marcel, C., de Vernal, A., Clark, P.U., Eby, M., 2004. Variation of Labrador Sea Water formation over the Last Glacial cycle in a climate model of intermediate complexity. Quaternary Science Reviews 23, 449–465.

de Abreu, L., Shackleton, N.J., Schönfeld, J., Hall, M., Chapman, M., 2003. Millennial-scale oceanic climate variability off the Western Iberian margin during the last two glacial periods. Mar. Geol. 196, 1–20.

de Vernal, A., Henry, M., Bilodeau, G., 1999. Techniques de préparation et d’analyse en micropaléontologie. Les cahiers du GEOTOP 3, 16-27.

de Vernal, A., Henry, M., Matthiessen, J., Mudie, P.J., Rochon, A., Boessenkool, K.P., Eynaud, F., Grøsfjeld, K., Guiot, J., Hamel, D., Harland, R., Head, M.J., Kunz-Pirrung, M., Levac, E., Loucheur, V., Peyron, O., Pospelova, V., Radi, T., Turon, J.-L., Voronina, E., 2001. Dinoflagellate cyst assemblages as tracers of sea-surface conditions in the Northern North Atlantic, Arctic and sub-Arctic seas: The new 'n = 677' data base and its application for quantitative palaeoceanographic reconstruction. Journal of Quaternary Sciences 16, 681-698.

de Vernal, A., Eynaud, F., Henry, M., Hillaire-Marcel, C., Londeix, L., Mangin, S., Matthiessen, J., Marret, F., Radi, T., Rochon, A., Solignac, S., Turon, J.L., 2005. Reconstruction of sea-surface conditions at middle to high latitudes of the Northern Hemisphere during the last glacial maximum (LGM) based on dinoflagellate cyst assemblages. Quat. Sci. Rev. 24, 897-924.

de Vernal, A., Rosell-Melé, A., Kucera, M., Hillaire-Marcel, C., Eynaud, F., Weinelt, M., Dokken, T., Kageyama, M., 2006. Comparing proxies for the reconstruction of LGM sea-surface conditions in the northern North Atlantic. Quaternary Science Reviews 25 (21-22), 2820-2834.

Duplessy, J.C., Shackleton, N.J., 1985. Response of global deep-water circulation to Earth's climate change 135,000 -107,000 years ago. Nature 316, 500-506.

Ehlers, J., Gibbard, P., 2004. Quaternary Glaciations: Extent and Chronology, Part 1: Europe. Developments in Quaternary Science, series 2A, Elsevier, 400 pp.

Elliot, M., Labeyrie, L., Bond, G., Cortijo, E., Turon, J.-L., Tisnerat, N., Duplessy, J.-C., 1998. Millennial-scale iceberg discharges in the Irminger Basin during the last glacial period: Relationship with the Heinrich events and environmental settings. Paleoceanography 13 (5), 433-446.

Elliot, M., Labeyrie, L., Dokken, T., Manthe, S., 2001. Coherent patterns of ice-rafted debris deposits in the Nordic regions during the last glacial (10-60 ka). Earth and Planetary Science Letters 194 (1-2), 151-163.

Esat, T.M., McCulloch, M.T., Chappell, J., Pillans, B., Omura, A., 1999. Rapid fluctuations in sea level recorded at Huon Peninsula during the penultimate deglaciation. Science 283 (5399), 197-201.

Everest, J.D., Bradwell, T., Fogwill, C.J. and Kubik, P.W., 2006. Cosmogenic 10BE age constraints for the Wester Ross Readvance moraine: Insights into British Ice-Sheet behaviour. Geografiska Annaler, Series A : Physical Geography 88 (1), 9-17.

Eynaud F., 1999. Kystes de Dinoflagellés et Evolution paléoclimatique et paléohydrologique de l'Atlantique Nord au cours du Dernier Cycle Climatique du Quaternaire. PhD, Bordeaux 1 Univ., 291 pp.

Eynaud, F., Turon, J.L., Sanchez-Goni, M.F., Gendreau, S., 2000. Dinoflagellate cyst evidence of "Heinrich-like events" off Portugal during the marine isotopic stage 5. Mar. Micropal. 40, 9-21.

Eynaud F., Turon J.L., Duprat J., 2004. Comparison of the Holocene and Eemian palaeoenvironments in the South-Icelandic basin: dinoflagellate cysts as proxies for the North Atlantic surface circulation. Review of Paleobotany and Palynology 128, 55-79.

Eynaud, F., Zaragosi, S., Scourse, J.D., Mojtahid, M., Bourillet, J.F., Hall, I.R., Penaud, A., Locascio, M. and Reijonen, A., 2007. Deglacial laminated facies on the NW European continental margin: the hydrographic significance of British Ice sheet deglaciation and Fleuve Manche paleoriver discharges. Geochemistry, Geophysics, Geosystems 8 (1), doi: 10.1029/2006GC001496.

Fensome, R.A., MacRae, R.A., Williams, G.L., 1998. DINOFLAJ. Geological Survey of Canada Open File, 3653.

Fensome, R.A., Williams, G.L., 2004. The Lentin and Williams index of fossil dinoflagellates, 2004 edition. AASP Foundation Contributions Series, vol. 42. 909 pp.

Flückiger, J., Knutti, R., White, J.W.C., 2006. Oceanic processes as potential trigger and amplifying mechanisms for Heinrich events. Paleoceanography 21 (2), 1-11.

Frew, R.D., Dennis, P.F., Karen, J.H., Michael, P.M., Steven, M.B., 2000. The oxygen isotope composition of water masses in the northern North Atlantic. Deep-Sea Res. Part 1, Oceanogr. Res. Pap. 47, 2265-2286.

Gallup, C.D., Cheng, H., Taylor, F.W., Edwards, R.L., 2002. Direct determination of the timing of sea level change during termination II. Science 295 (5553), 310-313.

Gibbard, P.L., Whiteman, C.A., Bridgland, D.R., 1988. A preliminary report on the stratigraphy of the Lower Thames Valley. Quaternary Newsletter 56, 1-8.

Grøsfjeld, K., Funder, S., Seidenkrantz, M.S., Glaister, C., 2006. Last Interglacial marine environments in the White Sea region, northwestern Russia. Boreas 35 (3), 493-520.

Grousset, F.E., Labeyrie, L., Sinko, J.A., Cremer, M., Bond, G., Duprat, J., Cortijo, E., Huon, S., 1993. Patterns of ice-rafted detritus in the Glacial North-Atlantic (40–50°N). Paleoceanography 8, 175–192.

Grousset, F.E., Pujol, C., Labeyrie, L., Auffret, G., Boelaert, A., 2000. Were the North Atlantic Heinrich events triggered by the behaviour of the European ice sheets? Geology 28, (2), 123-126.

Gupta, S., Collier, J.S., Palmer-Felgate, A., Potter, G., 2007. Catastrophic flooding origin of shelf valley systems in the English Channel. Nature 448, doi:10.1038/nature06018

Heinrich, H., 1988. Origin and consequences of cyclic ice rafting in the Northeast Atlantic Ocean during the past 130,000 years. Quat. Res. 29, 142–152.

Hemming, S.R., 2004. Heinrich events: massive late Pleistocene detritus layers of the North Atlantic and their global climate imprint. Rev. Geophys. 42, RG1005, doi: 10.1029/2003RG000128.

Henderson, G.M., Slowey, N.C., 2000. Evidence from U-Th dating against Northern Hemisphere forcing of the penultimate deglaciation. Nature 404, 61-66.

Hulbe, C.L., MacAyeal, D.R., Denton, G.H., Kleman, J., Lowell, T.V., 2004. Catastrophic ice shelf breakup as the source of Heinrich event icebergs. Paleoceanography 19 (1), 1-15.

Ivy-Ochs, S., Kerschner, H., Kubik, P.W., Schlüchter, C., 2006. Glacier response in the European Alps to Heinrich Event 1 cooling: The Gschnitz stadial. Journal of Quaternary Science 21 (2), 115-130.

Kaiser, J., 2001. Caractérisation palynologique des flux terrigènes Manche-Golfe de Gascogne au cours du Dernier Maximum Glaciaire et du réchauffement Holocène. Maîtrise des Sciences de l'Environnement, Univ. Bordeaux 1, Bordeaux, France, 30 pp.

Kempama, E.W., Reimnitz, E., Barnes, P.W., 2001. Anchor-ice formation and icerafting in southwestern Lake Michigan, U.S.A. Journal of Sedimentary Research 71, 346–354.

Knies, J., Vogt, C., Matthiessen, J., Nam, S.I., Ottesen, D., Rise, L., Bargel, T. and Eilertsen, R.S., 2007. Re-advance of the Fennoscandian Ice Sheet during Heinrich Event 1. Marine Geology 240 (1-4), 1-18.

Kucera, M., Weinelt, M., Kiefer, T., Pflaumann, U., Hayes, A., Weinelt, M., Chen, M.-T., Mix, A.C., Barrows, T.T., Cortijo, E., Duprat, J., Juggins, S., Waelbroeck, C., 2005. Reconstruction of sea-surface temperatures from assemblages of planktonic foraminifera: Multi-technique approach based on geographically constrained calibration data sets and its application to glacial Atlantic and Pacific Oceans. Quaternary Science Reviews 24 (7-9) SPEC. ISS., 951-998.

Lea, D.W., Martin, P.A., Pak, D.K., Spero, H.J., 2002. Reconstructing a 350 ky history of sea level using planktonic Mg/Ca and oxygen isotope records from a Cocos Ridge core. Quaternary Science Reviews 21 (1-3), 283-293.

Lebreiro, S.M., Moreno, J.C., McCave, I.N., Weaver, P.P.E., 1996. Evidence for Heinrich layers off Portugal. Mar. Geol. 131, 47–56.

Lericolais, G., 1997. Evolution du Fleuve Manche depuis l'Oligocène : stratigraphie et géomorphologie d'une plate-forme continentale en régime périglaciaire. Thèse de doctorat, Université Bordeaux 1, 265 pp.

Lericolais, G., Auffret, J.-P., Bourillet, J.-F., 2003. The Quaternary Channel River: Seismic stratigraphy of its palaeo-valleys and deeps. Journal of Quaternary Science 18 (3-4), 245-260.

Leymarie, M., 2008. Réponse de la végétation et du climat à la variabilité climatique du MIS 6 dans le Nord-Ouest de la Péninsule Ibérique. Master 2 ENVOLH, Univ. Bordeaux 1, Bordeaux, France, 30 pp.

Lézine, A.M., Duplessy, J.C., Cazet, J.P., 2005. West African monsoon variability during the last deglaciation and the Holocene: Evidence from fresh water algae, pollen and isotope data from core KW31, Gulf of Guinea. Palaeogeography, Palaeoclimatology, Palaeoecology 219, 225-237.

Lisiecki, L.E., Raymo, M.E., 2005. A Pliocene-Pleistocene stack of 57 globally distributed benthic δ 18O records. Paleoceanography 20 (1), 1-17.

Ludwig, K.R., Muhs, D.R., Simmons, K.R., Moore, J.G., 1992. Sr-isotope record of Quaternary marine terraces on the California coast and off Hawaii. Quaternary Research 37 (3), 267-280.

Major, C., Ryan, W., Lericolais, G., Hajdas, I., 2002. Constraints on Black Sea outflow to the Sea of Marmara during the last glacial-interglacial transition. Marine Geology 190 (1-2), 19-34.

Malaizé, B., Paillard, D., Jouzel, J., Raynaud, D., 1999. The Dole effect over the last two glacial-interglacial cycles. Journal of Geophysical Research D: Atmospheres 104 (D12, 27), 14199-14208.

Malaizé, B., Joly, C., Vénec-Peyré, M.-T., Bassinot, F., Caillon, N., Charlier, K., 2006. Phase lag between Intertropical Convergence Zone migration and subtropical monsoons onset over northwestern Indian Ocean during Marine Isotopic Substage 6.5 (MIS 6.5). Geochemistry, Geophysics, Geosystems 7, Q12N08, doi: 10.1029/2006GC001353.

Marret, F., 1994. Distribution of dinoflagellate cysts in recent marine sediments from the east Equatorial Atlantic (Gulf of Guinea). Review of Palaeobotany and Palynology 84, 1-22.

Marret, F, Eiríksson, J., Knudsen, K.L., Turon, J.-L., Scourse, J.D., 2004. Distribution of dinoflagellate cyst assemblages in surface sediments from the northern and western shelf of Iceland. Review of Palaeobotany and Palynology 128, 35-53.

Martinson, D.G., Pisias, N.G., Hays, J.D., Imbrie, J., Moore, T.C., Shackleton, N.J., 1987. Age dating and the orbital theory of the ICE Ages: development of a high resolution 0 to 300,000 year chronostratigraphy. Quat. Res. 27, 1-29.

Masson, V., Braconnot, P., Jouzel, J., De Noblet, N., Cheddadi, R., Marchal, O., 2000. Simulation of intense monsoons under glacial conditions. Geophysical Research Letters 27 (12), 1747-1750.

Matthiessen, J., 1995. Distribution patterns of dinoflagellate cysts and other organic-walled microfossils in recent Norwegian-Greenland Sea sediments. Mar. Micropal. 24, 307-334.

McCabe, A.M., Clark, P.U., Clark, J., 2007. Radiocarbon constraints on the history of the western Irish ice sheet prior to the Last Glacial Maximum. Geology 35 (2), 147-150.

McManus, J. F., Oppo, D. W., Cullen, J. L., 1999. A 0.5-Million-Year Record of Millennial-Scale Climate Variability in the North Atlantic. Science 283, 971-975.

McManus, J.F., Keigwin, L., Francois, R., Drown-Leger, S., Gherardi, J.M., 2004. Collapse and rapid resumption of Atlantic meridional circulation linked to deglacial climate changes, Nature, 428, 834–837.

Ménot, G., Bard, E., Rostek, F., Weijers, J.W.H., Hopmans, E.C., Scheuten, S., Sinninghe Damsté, J.S., 2006. Early reactivation of European rivers during the last deglaciation. Science 313 (5793), 1623-1625.

Mix, A.C., Bard, E., Schneider, R., 2001. Environmental processes of the ice age: Land, oceans, glaciers (EPILOG). Quaternary Science Reviews 20 (4), 627-657.

Mojtahid, M., Eynaud, F., Zaragosi, S., Scourse, J., Bourillet, J.F., Garlan, T., 2005. Palaeoclimatology and palaeohydrography of the glacial stages on Celtic and Armorican margins over the last 360 000 yrs. Marine Geology 224, 57-82.

Moros, M., Kuijpers, A., Snowball, I., Lassen, S., Bäckström, D., Gingele, F., McManus, J., 2002. Were glacial iceberg surges in the North Atlantic triggered by climatic warming? Marine Geology 192 (4), 393-417.

Mudie, P.J., Rochon, A., Aksu, A.E., 2002. Pollen stratigraphy of Late Quaternary cores from Marmara Sea: Land-sea correlation and paleoclimatic history. Marine Geology 190, 233-260.

Peck, V.L., Hall, I.R., Zahn, R., Elderfield, H., Grousset, F., Hemming, S.R., Scourse, J.D., 2006. High resolution evidence for linkages between NW European ice sheet instability and Atlantic Meridional Overturning Circulation. Earth and Planetary Science Letters 243 (3-4), 476-488.

Peck, V.L., Hall, I.R., Zahn, R., Grousset, F., Hemming, S.R., Scourse, J.D., 2007. The relationship of Heinrich events and their European precursors over the past 60 ka BP: a multi-proxy ice-rafted debris provenance study in the North East Atlantic. Quaternary Science Reviews 26 (7-8), 862-875.

Penaud, A., Eynaud, F., Turon, J.L., Zaragosi, S., Marret, F., Bourillet, J.F., 2008. Interglacial variability (MIS 5 and MIS 7) and dinoflagellate cyst assemblages in the Bay of Biscay (North Atlantic). Marine Micropaleontology 68, 136-155.

Pujol, C., Duprat, J., Gonthier, E., Moyes, J., Pujos-Lamy, A., 1973. Résultats préliminaires de l'étude effectuée par l'Institut de Géologie du Bassin d'Aquitaine sur les carottes prélevées dans le Golfe de Gascogne lors de la mission GESTLANTE IV (1ère partie 6 – 14 mars 1972). Bull. Inst. Geol. Bassin d'Aquitaine 13, 147-162.

Pujol, C., 1980. Les foraminifères planctoniques de l'Atlantique Nord au Quaternaire. Ecologie-Stratigraphie-Environnement. Mem. Inst. Geol. Bassin d'Aquitaine 10, 254.

Pujol, C., Zaragosi, S., Grousset, F., Paterne, M., Cortijo, E., Labeyrie, L., Manthé, S., Dennielou, B., Auffret, G.A., 2000. Age dating. In "ENAM II (1996-1999) European North Atlantic Margin".

Radi, T., de Vernal, A., 2004. Dinocyst distribution in surface sediments from the northeastern Pacific margin (40-60°N) in relation to hydrographic conditions, productivity and upwelling. Review of Paleobotany and Palynology 128, 169-193.

Rasmussen, T.L., Thomsen, E., Troelstra, S.R., Kuijpers, A., Prins, M.A., 2002. Millennial-scale glacial variability versus Holocene stability: changes in planktic and benthic foraminifera faunas and ocean circulation in the North Atlantic during the last 60 000 years. Marine Micropal. 47, 143-176.

Raymo, M.E., Ruddiman, W.F., Shackleton, N.J., Oppo, D.W., 1990. Evolution of Atlantic-Pacific δ13C gradients over the last 2,5 m.y. Earth Planet. Sci. Lett. 97, 353-368.

Reimnitz, E., Kempama, E.W., 1987. Field observations of slush-ice generated during freeze-up in Artic coastal waters. Marine Geology 77, 219–231.

Rochon, A., de Vernal, A., Turon, J.L., Matthiessen, J., Head, M.J., 1999. Recent dinoflagellate cysts of the North Atlantic Ocean and adjacent seas in relation to sea-surface parameters. 152 pp.

Rossignol-Strick, M., 1983. African monsoons, an immediate climate response to orbital insolation. Nature 304, 46-49.

Ruddiman, W.F., 1977. North Atlantic Ice-Rafting: A Major Change at 75,000 Years Before the Present. Science 196, 1208-1211.

Schmittner, A., 2005. Decline of the marine ecosystem caused by a reduction in the Atlantic overturning circulation. Nature 434, 628-633.

Schneider, R., Müller, P.-J., Acheson, R., 1999. Atlantic alkenone sea-surface temperature records, low versus mid latitudes and differences between hemispheres. In: Abrantes, F., Mix, A. C. (Eds.), Reconstructing ocean history: A window into the future. Plenum, New-York, pp 33-56.

Scourse, J.D., Hall, I.R., McCave, I.N., Young, J.R., Sugdon, C., 2000. The origin of Heinrich layers: evidence from H2 for European precursor events. Earth and Planetary Science Letters 182 (2), 187-195.

Snoeckx, H., Grousset, F., Revel, M., Boelaert, A., 1999. European contribution of ice-rafted sand to Heinrich layers H3 and H4. Marine Geology 158 (1-4), 197-208.

Spiegler, D., 1989. Ice-rafted Cretaceous and Tertiary fossils in Pleistocene-Pliocene sediments, ODP Leg 104, Norwegian Sea. Proceedings of the Ocean Drilling Program, Scientific Results, 104, 739-744.

Svendsen, J.I., Alexanderson, H., Astakhov, V.I., Demidov, I., Dowdeswell, J.A., Funder, S., Gataullin, V., Henriksen, M., Hjort, C., Houmark-Nielsen, M., Hubberten, H.W., Ingólfsson, O., Jakobsson, M., Kjær, K.H., Larsen, E., Lokrantz, H., Lunkka, J.P., Lysa, A., Mangerud, J., Matiouchkov, A., Murray, A., Möller, P., Niessen, F., Nikolskaya, O., Polyak, L., Saarnisto, M., Siegert, C., Siegert, M.J., Spielhagen, R.F., Stein, R., 2004. Late Quaternary ice sheet history of northern Eurasia. Quat. Sci. Rev. 23 (11-13), 1229-1271.

Tian, J., Brown, T.A., Hu, F.S., 2005. Comparison of varve and 14C chronologies from Steel Lake, Minnesota, USA. Holocene 15, 510-517.

Tisserand, A., Malaizé, B., Jullien, E., Zaragosi, S., Charlier, K., Grousset, F., 2009. African monsoon enhancement during the penultimate glacial period (MIS 6.5 ~ 170 ka) and its atmospheric impact. Paleoceanography 24, PA2220, doi:10.1029/2008PA001630.

Toucanne, S., Zaragosi, S., Bourillet, J.F., Naughton, F., Cremer, M., Eynaud, F., Dennielou, B., 2008. Activity of the turbidite levees of the Celtic-Armorican margin (Bay of Biscay) during the last 30,000 years: Imprints of the last European Deglaciation and Heinrich events. Marine Geology 247 (1-2), 84-103.

Toucanne S., Zaragosi, S., Bourillet, J.F., Cremer, M., Eynaud, F., van Vliet-Lanoe, B., Penaud, A., Fontanier, C., Turon, J.L., Cortijo, E., Gibbard, P.L., 2009. Timing of massive ‘Fleuve Manche’ discharges over the last 400 kyr: insights into the European Ice Sheet oscillations and the European drainage network from MIS 10 to 2. Quaternary Science Reviews 28 (13-14), 1238-1256.

Turon, J.-L., 1984. Le palynoplancton dans l'environnement actuel de l'Atlantique Nord-oriental. Evolution climatique et hydrologique depuis le dernier maximum glaciaire. Mémoires de l'Institut de Géologie du Bassin d'Aquitaine 17, 313 pp.

Turon, J.-L., Londeix, L., 1988. (Dinoflagellate assemblages in the western Mediterranean, Alboran sea: evidence of the evolution of palaeoenvironments since the last glacial maximum). [Les assemblages de kystes de Dinoflagelles en Mediterranee occidentale (Mer d'Alboran) : mise en evidence de l'evolution des paleoenvironnements depuis le dernier maximum glaciaire.]. Bulletin – Centres de Recherche Exploration-Production Elf- Aquitaine, 12 (1), 313-344.

Turon, J.-L., Lézine, A.-M., Denèfle, M., 2003. Land–sea correlations for the last glaciation inferred from a pollen and dinocyst record from the Portuguese margin. Quaternary Research 59, 88–96.

Vidal, L., Labeyrie, L., Cortijo, E., Arnold, M., Duplessy, J.C., Michel, E., Becqué, S., van Weering, T.C.E., 1997. Evidence for changes in the North Atlantic Deep Water linked to meltwater surges during the Heinrich events. Earth Planet. Sci. Lett. 146, 13-27.

Waelbroeck, C., Labeyrie, L., Michel, E., Duplessy, J. C., McManus, J. F., Lambeck, K., Balbon, E., Labracherie, M., 2002. Sea-level and deep water temperature changes derived from benthic foraminifera isotopic records. Quaternary Science Reviews 21 (1-3), 295-305.

Weldeab, S., Emeis, K.C., Hemleben, C., Schmiedl , G., Schulz, H., 2003. Spatial productivity variations during formation of sapropels S5 and S6 in the Mediterranean Sea: evidence from Ba contents. Palaeogeography, Palaeoclimatology, Palaeoecology 191, 169-190.

Winograd, I.J., Coplen, T.B., Landwehr, J.M., Riggs, A.C., Ludwig, K.R., Szabo, B.J., Kolesar, P.T., Revesz, K.M., 1992. Continuous 500,000-year climate record from vein calcite in Devils Hole, Nevada. Science 258 (5080), 255-260.

Winograd, I.J., Landwehr, J.M., Ludwig, K.R., Coplen, T.B., Riggs, A.C., 1997. Duration and structure of the past four interglaciations. Quaternary Research 48 (2), 141-154.

Zaragosi, S., Eynaud, F., Pujol, C., Auffret, G.A., Turon, J.L., Garlan, T., 2001. Initiation of European deglaciation as recorded in the northwestern Bay of Biscay slope environments (Meriadzek Terrace and Trevelyan Escarpment): a multi-proxy approach. Earth Planet. Sci. Lett. 188, 493-507.

Zaragosi, S., Bourillet, J.-F., Eynaud, F., Toucanne, S., Denhard, B., van Toer A., Lanfumey, V., 2006. The impact of the last European deglaciation on the deep-sea turbidite systems of the Celtic-Armorican margin (Bay of Biscay). Geo-Marine Letters 26 (6), 317-329.

Zonneveld, K.A.F., Hoek R.P., Brinkhuis, H., Willems, H., 2001. Geographical distributions of organic-walled dinoflagellate cysts in surficial sediments of the Benguela upwelling region and their relationship to upper ocean conditions. Progress in Oceanography 48, 25-72.

9. Tables and Figure legends

	Concentrations (Cysts or *Pediastrum* / cm^3)		
	***Pediastrum* spp.**	**Md dinocysts**	**Rd dinocysts**
MIS 2 laminae	271	960	1304
MIS 6 laminae	286	504	2286
MIS 6 / MIS 2 laminae	**1.1**	**0.5**	**1.8**
MIS 2 and MIS 6 (except laminae)	139	8226	405

Table 1: Comparison of MIS 2 termination with mid-MIS 6 laminated deposits: average of *Pediastrum* spp. coenobia concentrations, Modern (Md) and Reworked (Rd) dinocyst concentrations, as well as ratio "Reworked versus Modern dinocysts" (Rd/Md). The ratio MIS 2/MIS 6 enables quantification of the difference in terms of reworked tracer concentrations and of dinocyst productivity in between the two laminated intervals. "MIS 2 and MIS 6 (except laminae)" represents the average of palynomorph concentrations in core MD03-2692, except for those recorded during the laminated events.

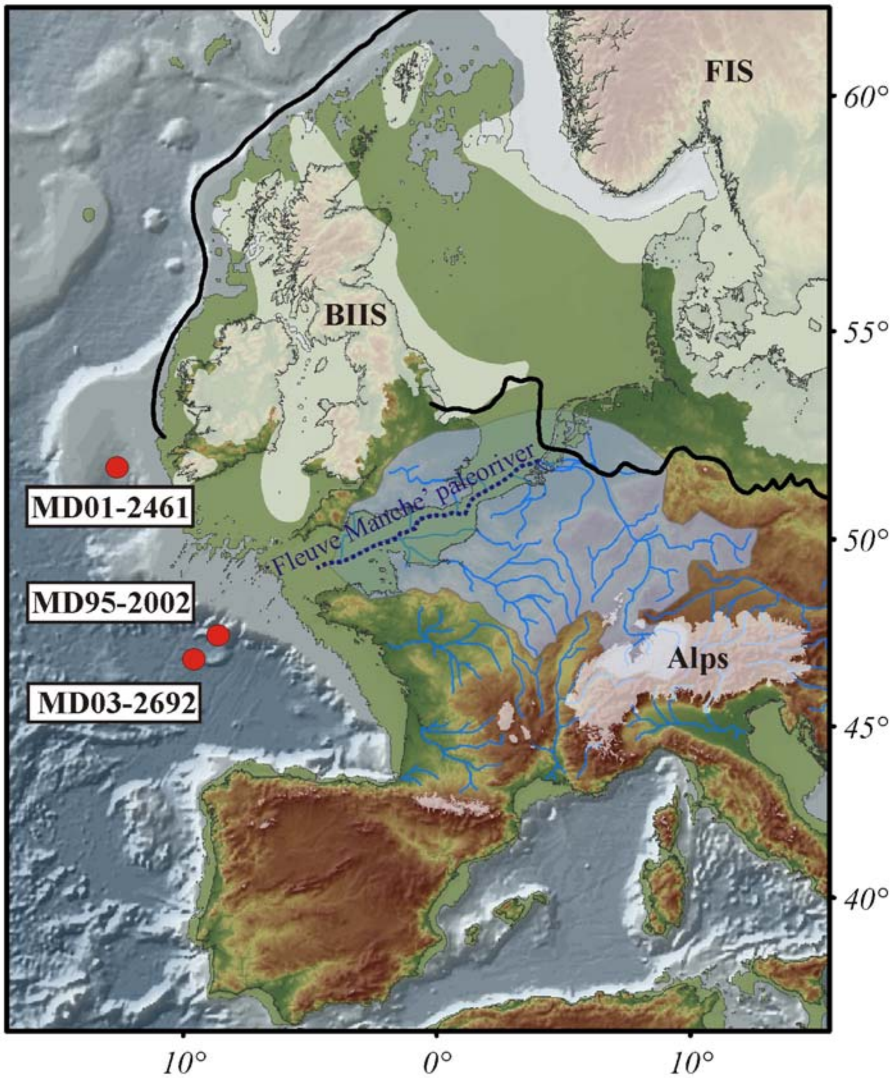

Figure 1: Paleogeographic reconstruction of NW Europe during the Late Weichselian (MIS 2) and Saalian glaciations (MIS 6). British Irish Ice Sheet (BIIS) margins, Fennoscandian Ice Sheet (FIS) and the Alps Glaciers are taken from Svendsen et al. (2004) and Ehlers and Gibbard (2004); the white colour delimits the BIIS during MIS 2 and the thick dark line delimits the extent of the BIIS during MIS 6. Blue lines represent the drainage basin and the main European rivers, taken from Major et al. (2002) and Bourillet et al. (2003). The 'Fleuve Manche' paleoriver is represented with a dark blue dotted line, and its surrounding drainage basin is lightened on the map. Bathymetry and altimetry correspond to the ETOPO2 (http://www.ngdc.noaa.gov/mgg/fliers/01mgg04.html) and SRTM (Global Land Cover Facility, http://www.landcover.org) data, respectively. Sea-level is lowered 120 m everywhere such as the LGM configuration. Therefore, the part of the shelf emerging at that time is represented in

light green. The studied core MD03-2692 (46°50'N, 9°31'W, 4064 m water depth, Trevelyan Escarpment), as well as core MD95-2002 (47°27'N, 08°32'W, 2174 m water depth, Meriadzek Terrace) and core MD01-2461 (51.75°N, 12.55°W, 1153 m water depth, Western Porcupine Bight), discussed in the paper, are located on the map.

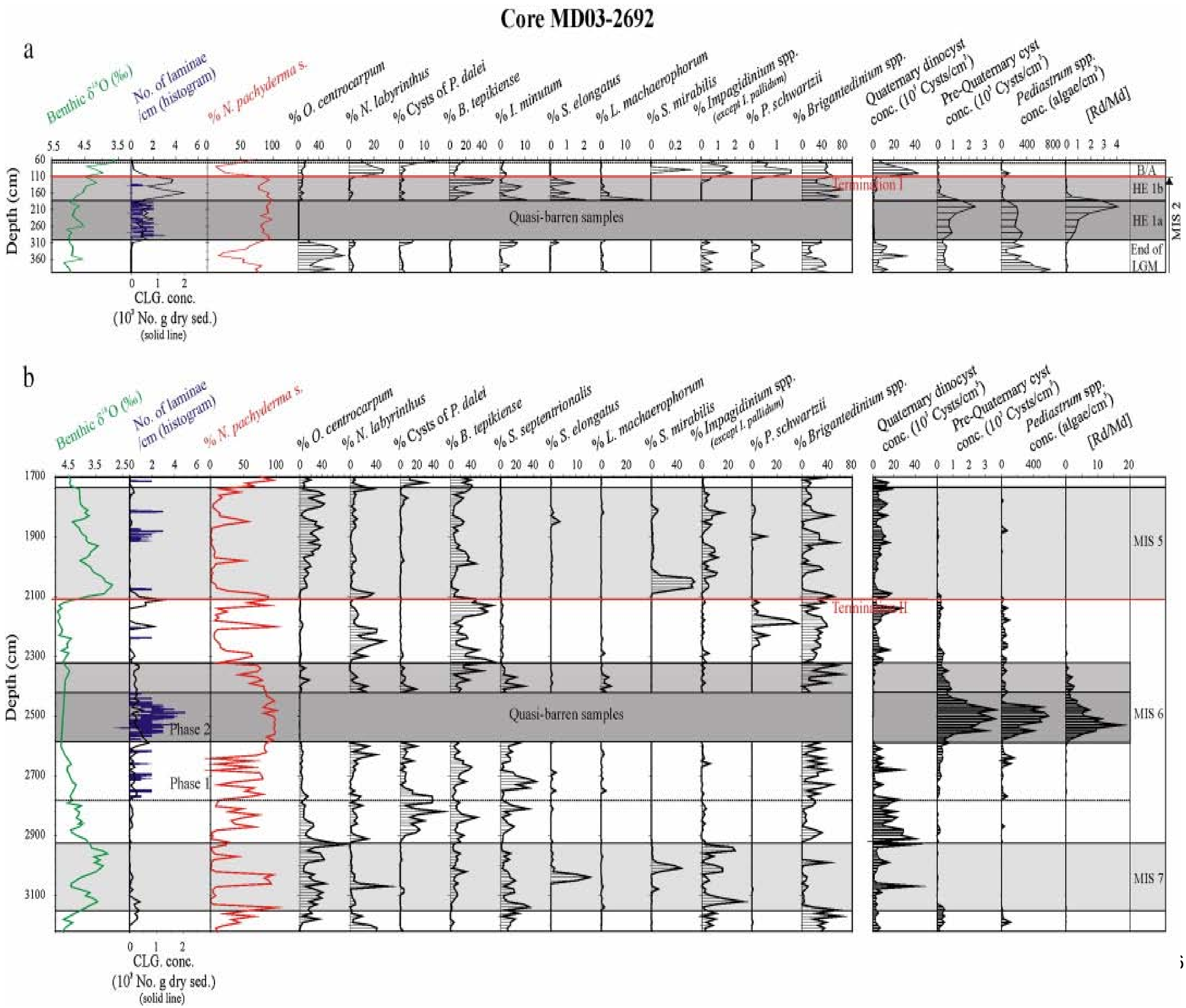
Core MD03-2692
a
Benthic δ18O (‰)
No. of laminae /cm (histogram)
% N. pachyderma s.
% O. centrocarpum
% N. labyrinthus
% Cysts of P. dalei
% B. tepikiense
% I. minutum
% S. elongatus
% L. machaerophorum
% S. mirabilis
% Impagidinium spp. (except I. pallidum)
% P. schwartzii
% Brigantedinium spp.
Quaternary dinocyst conc. (10³ Cysts/cm³)
Pre-Quaternary cyst conc. (10³ Cysts/cm³)
Pediastrum spp. conc. (algae/cm³)
[Rd/Md]
Depth (cm)
Quasi-barren samples
Termination I
B/A
HE 1b
HE 1a
End of LGM
MIS 2
CLG. conc. (10³ No. g dry sed.) (solid line)
b
Benthic δ18O (‰)
No. of laminae /cm (histogram)
% N. pachyderma s.
% O. centrocarpum
% N. labyrinthus
% Cysts of P. dalei
% B. tepikiense
% S. septentrionalis
% S. elongatus
% L. machaerophorum
% S. mirabilis
% Impagidinium spp. (except I. pallidum)
% P. schwartzii
% Brigantedinium spp.
Quaternary dinocyst conc. (10³ Cysts/cm³)
Pre-Quaternary cyst conc. (10³ Cysts/cm³)
Pediastrum spp. conc. (algae/cm³)
[Rd/Md]
Depth (cm)
Quasi-barren samples
Termination II
Phase 2
Phase 1
MIS 5
MIS 6
MIS 7
CLG. conc. (10³ No. g dry sed.) (solid line)

Figure 2: Core MD03-2692. Micropaleontological (Dinoflagellate cysts assemblages; Quaternary and pre-Quaternary dinocyst concentrations; *Pediastrum* spp. coenobia concentrations; and ratio Reworked versus Modern dinocysts: Rd/Md), geochemical, and sedimentological data obtained in between MIS 5 and MIS 7 (b), and during the end of MIS 2 (a). Core depths are displayed in centimetres along the vertical axis. Relative abundances of the dominant dinoflagellate cysts species are compared with *N. pachyderma* sinistral percentages, the number of laminae per centimetre, Coarse Lithic Grain concentrations (CLG. conc.), as well as the benthic oxygen isotope curve providing the stratigraphical framework for the core. Marine Isotope Stages (MIS) are indicated at the right of the diagram.
LGM: Last Glacial Maximum; HE 1a: First part of Heinrich Event 1 with laminae; HE 1b: Second part of Heinrich event 1 without laminae; B/A: Bölling/Allerod. The cold event within mid-MIS 6 around 2,500 cm depth, similar to that occurring during HE 1, is also divided into two parts represented by gray bands. The first part marked by laminated sediments is underlined by a darker gray band.

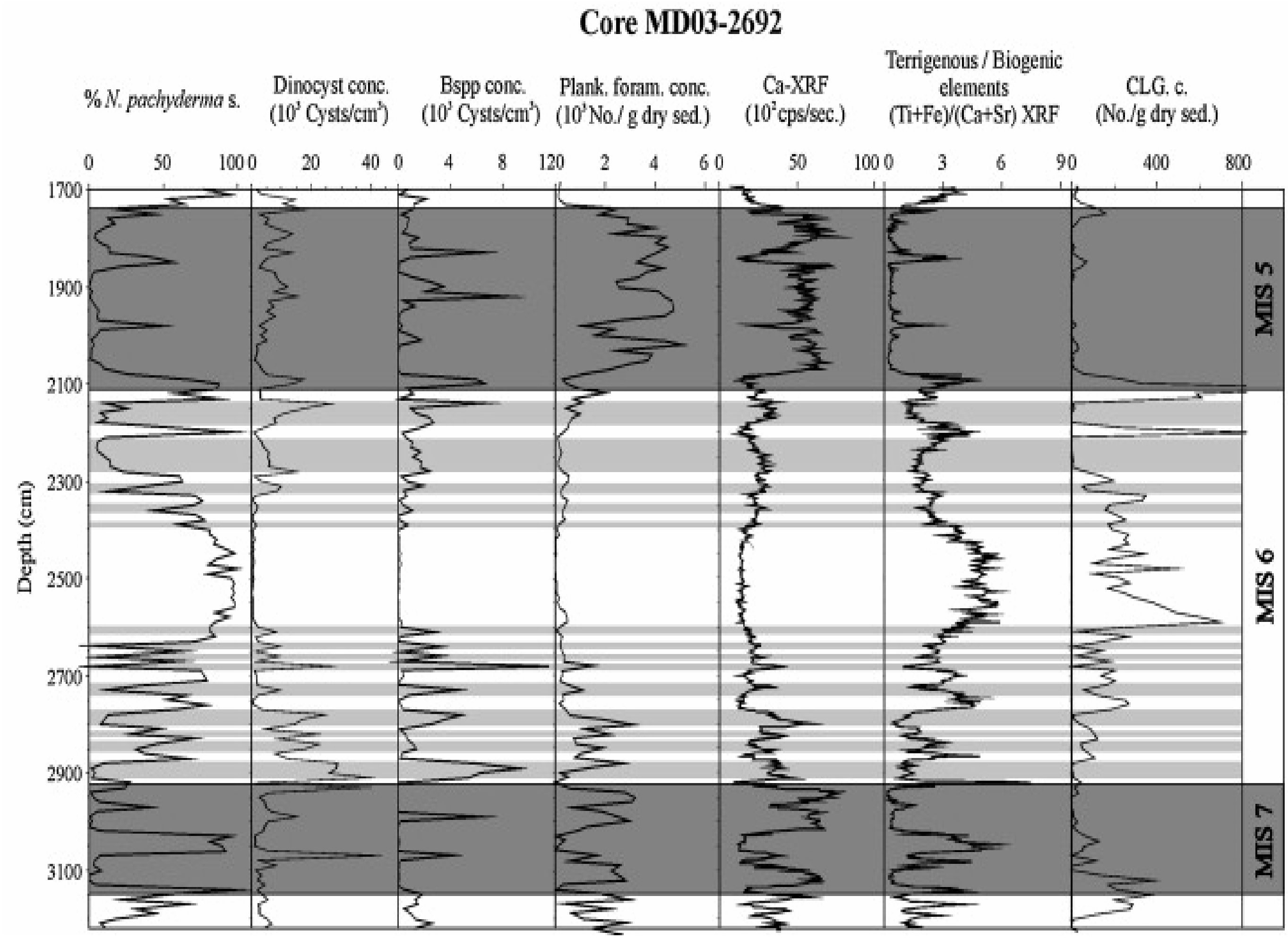

Figure 3: Core MD03-2692. Synthetic figure summarizing some results, obtained between MIS 7 and MIS 5, plotted along depth in the core: Relative abundances of the polar foraminifera *N. pachyderma* s., *Brigantedinium* spp. (Bspp) concentrations, Quaternary dinocyst concentrations, planktonic foraminifera concentrations, records obtained by XRF (Calcium, and ratio terrigenous (Ti and Fe) versus biogenic (Ca and Sr) elements), Coarse Lithic Grain concentrations (CLG. c.). Dark gray bands mark the last and penultimate Interglacial Complexes (MIS 5 and MIS 7, respectively) and bright gray bands mark warmer intervals through the glacial MIS 6.

a) MIS 2 laminae - core MD03-2692 (Mojtahid et al., 2005; this work)

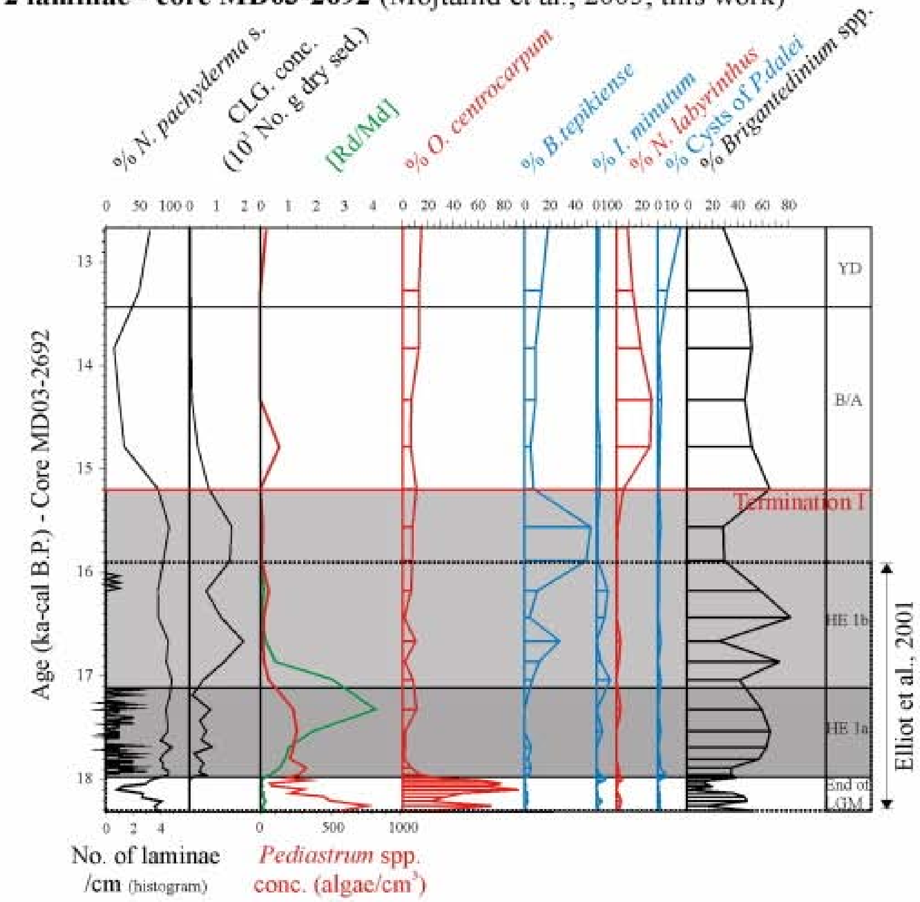

b) MIS 2 laminae - core MD95-2002 (Zaragosi et al., 2001)

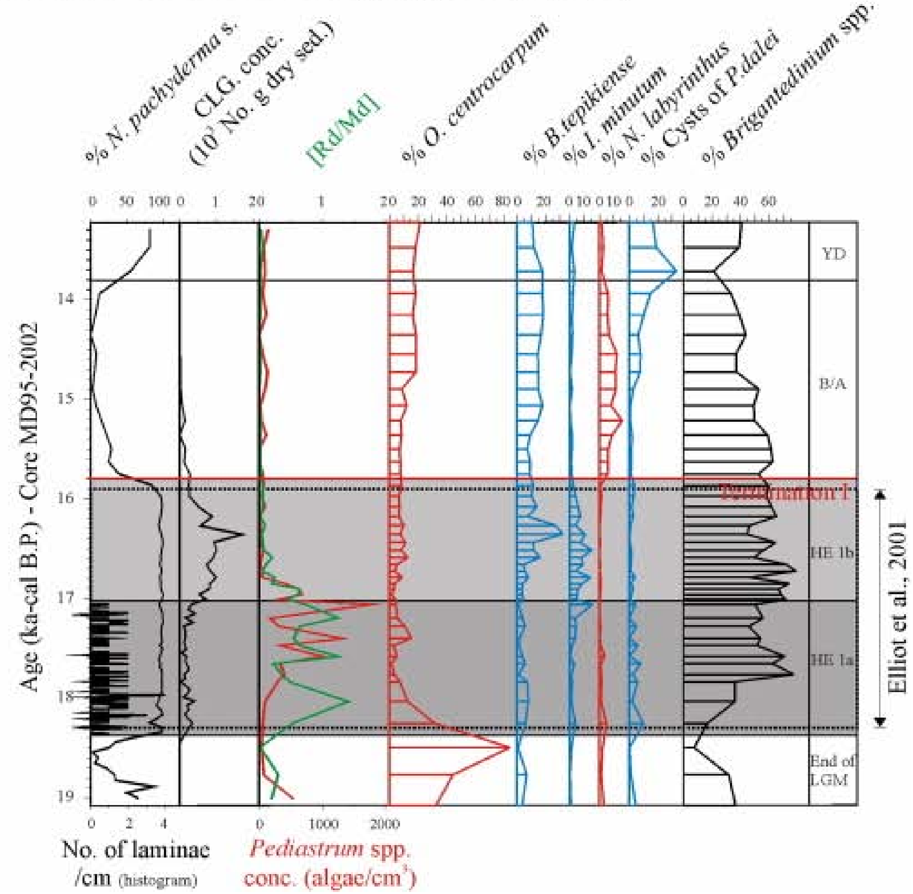

Figure 4: Records in ka calendar B.P. obtained on two proximal cores from the Bay of Biscay, MD03-2692 (a) and MD95-2002 (b) between the end of the Last Glacial Maximum and the start of the Younger Dryas. Comparison of the number of laminae per centimetre with Coarse Lithic Grain concentrations (CLG. Conc.), relative abundances of *Neogloboquadrina pachyderma* s., as well as relative abundances of selected dinocysts taxa (*Operculodinium centrocarpum, Bitectatodinium tepikiense, Islandinium minutum, Nematosphaeropsis labyrinthus,* cysts of *Pentapharsodinium dalei, and Brigantedinium* spp.*)*, *Pediastrum* spp. coenobia concentrations, and ratio Reworked versus Modern dinocysts: Rd/Md. Heinrich Event 1 boundaries are deduced from the plateau of *N. pachyderma* s. in both cores. The dates given in the North Atlantic by Elliot et al. (1998, 2001) for HE 1, between 18.3 and 15.9 ka cal B.P., are placed on each figure.
LGM: Last Glacial Maximum; HE 1a: first part of Heinrich Event 1 with laminae; HE 1b: second part of Heinrich event 1 without laminae; B/A: Bölling/Allerod; YD: Younger Dryas.

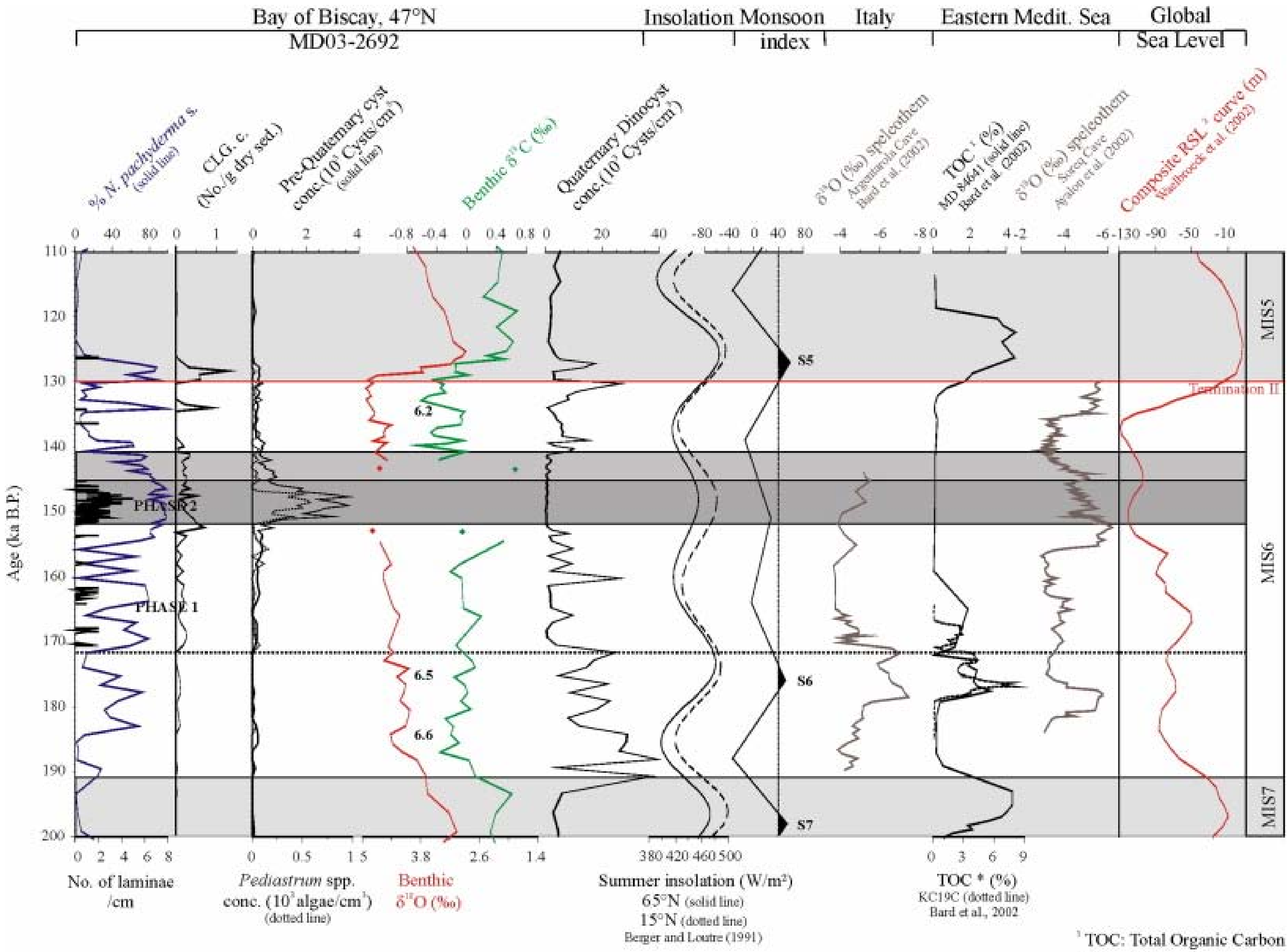

¹ TOC: Total Organic Carbon

² RSL: Relative Sea Level

Figure 5: Multiproxy compilation plotted against age (ka B.P.) of some selected results acquired in core MD03-2692 compared with results obtained on different cores retrieved through the Mediterranean Basin, versus July Insolation curves at 65°N and 15°N (Berger and Loutre, 1991), and the composite relative sea-level (RSL) curve established by Waelbroeck et al. (2002). For the Monsoon index established by Rossignol-Strick (1983), a sapropel (S) is formed every time the index is above the threshold value of 41; it corresponds here to S5, S6, and S7. The cold event within mid-MIS 6, around 150 ka B.P., is divided into two parts represented by gray bands. The first part marked by laminated sediments is underlined by a darker gray band. Isotopic events 6.6 (183 ka B.P.), 6.5 (175 ka B.P.), and 6.2 (135 ka B.P.) are placed along the benthic oxygen curve according to Martinson et al. (1987).